The Canadian Journal of Chemical Engineering

formerly

CANADIAN JOURNAL OF TECHNOLOGY

CONTENTS

Published by
THE CHEMICAL INSTITUTE OF CANADA
OTTAWA CANADA

A Pigmy Paper-maker

turns out samples at the C-I-L Central Research Laboratory at Beloeil, Que. The products of this miniature paper mill are used to study bleaching of various types of wood pulp with C-I-L chemicals. The findings of the studies are made available to the pulp and paper industry through the technical service representatives of C-I-L.

C-I-L research helps many other industries to develop the improved products Canada needs for progress.

C-I-L

CANADIAN INDUSTRIES LIMITED

Serving Canadians Through Chemistry

Agricultural Chemicals • Ammunition • Coated Fabrics – Industrial Chemicals • Commercial Explosives • Paints • Plastics • Textile Fibres

The Canadian Journal of Chemical Engineering

formerly

Canadian Journal of Technology

VOLUME 36 | OCTOBER, 1958 | NUMBER 5

Authorized as second class mail, Post Office Department, Ottawa. Printed in Canada

Manuscripts for publication should be submitted to the Editor: Dr. W. M. Campbell, Chemistry and Metallurgy Division, Atomic Energy of Canada Limited, Chalk River, Ontario. (Instruction to authors are on inside back cover)

Proofs, correspondence concerning proofs, and orders for reprints should be sent to: The Chemical Institute of Canada, 18 Rideau Street, Ottawa 2, Ont.

Subscriptions, renewals, requests for single or back numbers and all remittances should be sent to: The Chemical Institute of Canada, 18 Rideau Street, Ottawa 2, Ont.

C.J.Ch.E. is published by The Chemical Institute of Canada every two months. Subscription rate is $3.00 per year and .75c per single copy; U.S. and U.K.–$4.00; and Foreign–$4.50 per year.

Editorial Offices: Dr. W. M. Campbell, Chemistry and Metallurgy Division, Atomic Energy of Canada Limited, Chalk River, Ont.

Production and circulation offices: 18 Rideau Street, Ottawa 2, Ont.

Change of Address: Advise the Circulation Department, The Chemical Institute of Canada, 18 Rideau Street, Ottawa 2, Ont. in advance of any change of address, providing old as well as new address. Enclose address label if possible.

The Upward Vertical Flow of Air-Water Mixtures[1]

II. Effect of Tubing Diameter on Flow Pattern, Holdup and Pressure Drop

G. W. GOVIER[2] and W. LEIGH SHORT[3]

Results of visual observations and measurements of holdup and pressure drop are reported over a range of air-water ratios for the upwards vertical flow of air-water mixtures in four tubes with diameters ranging from 0.630 in. to 2.50 in. Tests were conducted under conditions of constant air density corresponding with an average pressure of 36 psia and at 10 constant superficial water velocities ranging from 0.0695 to 7.35 ft./sec.

The data are analyzed by the method previously suggested by Govier, Radford and Dunn involving the separation of the unit pressure drop curves into four regimes to aid in flow pattern description and the separation of the unit pressure drop itself into two components to facilitate correlation.

Tubing diameter is found to have little or no effect on the border between Regimes I and II or on the transition from the bubble to the slug flow pattern. The borders between Regimes II and III and between Regimes III and IV are markedly affected by tubing diameter as by consequence are the transitions from slug to froth and from froth to ripple flow.

Tubing diameter is found to have an important effect on the superficial friction factor and the holdup. The pressure drop data for each of the diameters have been successfully brought together in a single friction factor-Reynolds number correlation. The holdup data are separately correlated for pressure drop Regimes I and II and for Regime III and Regime IV.

THE first paper [1] of this series presented a review of the general characteristics of the upwards vertical flow of gas-liquid mixtures and indicated the complex flow patterns and the existence of holdup both of which distinguish the flow of two phase mixtures from that of single phase fluids. A comparison of the flow pattern nomenclature employed by other workers led to the proposal of the terms "bubble", "slug", "froth", "ripple", "film" and "mist" for the identifiable patterns encountered at constant liquid flow rate with increasing ratio of the gas to liquid phase. These flow patterns were identified with some precision and correlated with the aid of the loci of inflection points in the relationships between the unit pressure drop and the volume ratio of the phases. Holdup (which is related to "slip velocity") was expressed quantitatively in terms of holdup ratio, H_R, defined as the ratio between (a) the gas-liquid volume ratio in the supply mixture and (b) the gas-liquid volume ratio in the flow section. This holdup ratio was correlated in terms of the superficial velocity of the liquid phase and the volume ratio of the phases.

In a thermodynamic analysis of the problem the overall unit pressure drop was separated into its two basic components—that due to the hydrostatic head and that due to the irreversibilities attending flow. The equation expressing this relationship, in terms of feet of liquid phase per foot of height, is:

$$-v_L \frac{\Delta P}{\Delta X} = \frac{1 + R_M}{1 + R_V} + \frac{1}{1 + R_V}\left(\frac{\Delta F}{\Delta X}\right)_L \quad \ldots\ldots\ldots (1)$$

where

v_L = specific volume of liquid, ft³/lb
$-\Delta P$ = pressure drop, lbs/ft²
ΔX = incremental height, ft
R_M = gas-liquid mass ratio, $\frac{G}{L}$
R_V = gas-liquid volume ratio, $\frac{Gv_G}{Lv_L}$
$\left(\frac{\Delta F}{\Delta X}\right)_L$ = irreversibility effect, feet of liquid per foot of height

The quantity $\left(\frac{\Delta F}{\Delta X}\right)_L$ may conveniently be expressed in terms of f'_L, a superficial friction factor based upon the liquid phase, by the relationship:

$$\left(\frac{\Delta F}{\Delta X}\right)_L = \frac{2 f'_L V_L^2}{g_c D} \quad \ldots\ldots\ldots\ldots\ldots (2)$$

where

V_L = the superficial liquid phase velocity based upon the total tube cross section, ft./sec.
g_c = dimensional conversion factor, $lb._M ft./lb._F sec.^2$
D = tube diameter, ft.

This latter equation serves to define the superficial friction factor, f'_L, which may be expected to depend upon a superficial Reynolds number, and some function of the system geometry, the fluid properties and the mass or volume ratio of the two phases. The work previously reported has indicated that experimental pressure data may in fact be so correlated.

The correlations of the flow pattern, holdup and pressure drop data referred to, however, are limited in applications to the conditions of the experimental data. The data presented in Part I are for the air-water system flowing in a smooth bore 1.025 in. I.D. tube at water rates ranging from 0.00040 to 0.0421 cu. ft./sec. and at air-water volume ratios ranging from 0 to 348. The properties of both phases were held constant through the maintenance of constant average flowing pressure and temperature of

[1]*Manuscript received July 10, 1958.*
[2]*Head, Department of Chemical and Petroleum Engineering, University of Alberta, Edmonton, Alta.*
[3]*Project Engineer, Plastics Division, Canadian Industries Limited, Edmonton, Alta.*
Contribution from the Department of Chemical and Petroleum Engineering, University of Alberta, Edmonton, Alta. and presented at the Joint A.I.Ch.E.-C.I.C. Chemical Engineering Conference, Montreal, April 20-23, 1958.

36.0 psia and 85°F. The work reported here was undertaken to shed light on the effect of tubing diameter. Other work now under way and to be reported later has been designed to clarify the role of liquid and gas phase properties.

Experimental equipment and procedure

The equipment employed for the tests reported here and illustrated in Figure 1 is essentially the same as that described in Part I. It was modified by the incorporation of three additional flow sections to give the following each of 22.88 ft. effective length:

(a) a 0.630 in. I.D. smooth bore transparent cellulose-acetate-butyrate tube,
(b) the original 1.025 in. I.D. smooth bore transparent cellulose-acetate-butyrate tube,
(c) a 1.50 in. I.D. smooth bore seamless copper tube, and
(d) a 2.50 in. I.D. smooth bore opaque carbon black loaded polythene tube.

Suitable carefully reamed pressure taps were made in the new tubes at elevations corresponding to that in the original tube.

The data taking procedure was almost exactly as previously reported, but flow patterns were identified primarily from the inflection points. Tests were conducted at superficial water velocities at and near 0.0695, 0.135, 0.295, 0.625, 0.869, 1.50, 2.05, 2.51 and 3.47 ft./sec. corresponding to those previously made in the 1.025 in. tube. The average flowing pressure was held constant at 36.0 psia and the temperature was held nearly constant in the range 70°-85°F.

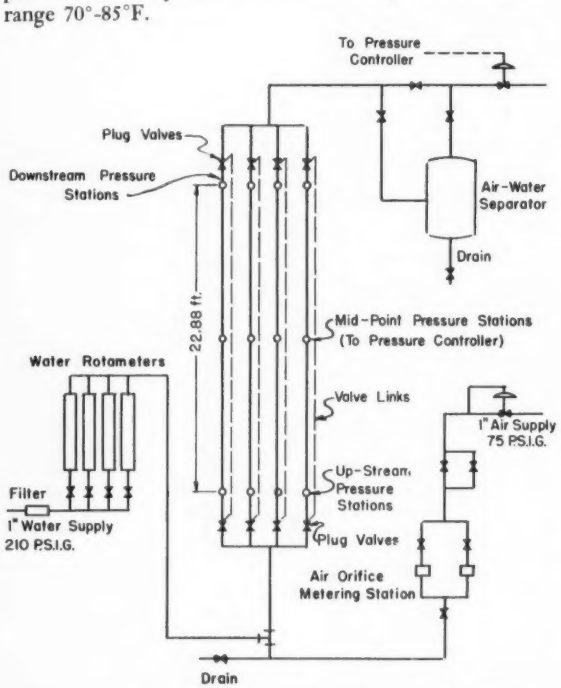

Figure 1—Schematic flow diagram of equipment.

Experimental results

The basic experimental data are tabulated in Table I (Partial) for the typical constant water rate of some 0.87 ft./sec. The complete tabular data for all water rates is given in Table 1 deposited as Document No. 5723* with the American Documentation Institute Auxiliary Publication Project, Photo Duplication Service, Library of Congress, Washington 25, D.C. For convenience the data from Part I for the 1.025 in. tube at the 0.873 ft./sec. velocity is repeated in Table I (Partial).

Referring to Table I (Partial), column 2 gives the tube diameter, column 3 gives the water rate in cubic feet per second, column 4 the water-saturated air rate in cu. ft./sec. at the mid-point temperature given by column 5 and the constant mid-point pressure of 36.0 psia. These rates were calculated from the actual measured air rates to correct for the saturation of the air with water which took place in the calming section. Column 6 presents the ratio of the air to water rates on a volume basis. Column 7 gives the volume ratio of air to water trapped in the test section at the completion of each test. Column 8 gives the specific volume of the saturated air at mid-point test section conditions. Column 9 presents the holdup ratio, being the ratio of the discharge air-water volume ratio to the test section air-water volume ratio i.e. of column 6 to column 7. Column 10 gives the total pressure drop between the upstream and downstream pressure measuring stations, expressed in terms of ft. of water per ft. of height. Column 11 identifies the pressure drop regime and Column 12 the flow pattern.

The basic data for the 0.630, the 1.50 and the 2.50 in. I.D. tubes at each of the water rates tested are summarized in Figures 2 through 18. These figures show by separate curves (a) the relationship between the unit pressure drop and the air-water volume ratio at test conditions and (b) the relationship between holdup ratio and air water volume ratio at test conditions. The four pressure drop regimes defined in Part I for the 1.025 in. tube are clearly distinguishable in Figures 2, 3, 4 and 12, perceptible in Figures 5, 6 and 11, and partially apparent in Figures 7 to 10, and 13 to 18. As previously found the data for the higher water rates indicates a narrowing of Regime III and a merging of Regimes II and IV. Thus for the 0.630 in. tube all four regimes are apparent at a superficial water velocity of 0.624 ft./sec., Regime III is barely perceptible at the velocity of 2.04 ft./sec. and it has disappeared completely and Regimes II and IV have merged at the velocity of 3.47 ft./sec. Similar observations were reported for the 1.025 in. tube with the velocity at disappearance of Regime III being about 3.5 ft./sec. In the case of the 1.5 in. tube Regimes I, II and III are clearly apparent up to water velocity of 2.50 ft./sec., although only at that water velocity were sufficiently high air rates realized to illustrate Regime IV. Insufficiently high air rates were obtained at the water rate of 3.47 ft./sec. definitely to determine the presence of Regimes II, III or IV, although the correlation to be described later suggests that Regime III is actually missing and that Regimes II and IV are merged. With the 2.50 in. tube Regimes I, II and III are apparent to water velocities of 2.05 ft./sec., although Regime III becomes increasingly indistinct as the water velocity is increased. It is clear that the disappearance of Regime III and the mergence of Regimes II and IV takes place at different water and air velocities in the tubes of different diameter.

The general shape of the holdup curve is more or less the same for all diameters and all superficial water velocities. The holdup ratio is unity (slip velocity is zero) at zero air-water ratio, it increases with air-water volume ratio passing through an inflection point about in the middle of Regime I, and thereafter increases to a second inflection point near the end of Regime II, after which it increases more slowly, levels or decreases.

*A more detailed form of this paper has been deposited as Document No. 5723 with the ADI Auxiliary Publications Project, Photoduplication Service, Library of Congress, Washington 25, D.C. A copy may be secured by citing the Document No. and by remitting $1.25 for photoprints, or $1.25 for 35 mm. microfilm. Advance payment is required. Make checks or money orders payable to: Chief, Photoduplication Service, Library of Congress.

TABLE 1 (PARTIAL)

EXPERIMENTAL DATA

Test Section Length 22.88 Ft.
Test Section Mid Point Pressure 36.0 Psia
Test Section Mid Point Temperature as Indicated
Specific Volume of Liquid Phase = 0.01603 Ft^3/Lb
Specific Volume of Saturated Gas Phase as Indicated
Superficial Water Velocities Approximately Constant at 0.850–0.873 ft/sec.

(1)	(2)	(3)	(4)	(5)	(6)	(7)	(8)	(9)	(10)	(11)	(12)
Test Number	Tube Diameter inches	Water Rate ft^3/sec	Saturated Air Rate ft^3 sec*	Mid Point Temperature °F	Discharge Air-Water Ratio**	Test Section Air-Water Ratio	Specific Volume Saturated Gas Phase ft^3/lb	Holdup Ratio***	Pressure Drop ft H_2O/ft	Pressure Drop Regime	Flow Pattern
280D	0.630	0.00183	.00426	62	2.33	1.29	5.37	1.81	0.413	I	Slug
281D	0.630	0.00183	.00574	62	3.14	1.73	5.37	1.82	0.348	I	Slug
282D	0.630	0.00183	.00828	62	4.52	2.12	5.37	2.13	0.300	I	Slug
283D	0.630	0.00183	.0155	63	8.47	2.71	5.38	3.13	0.300	II	Slug
284D	0.630	0.00183	.0230	63	12.6	2.79	5.38	4.52	0.330	II	Froth
285D	0.630	0.00183	.0281	64	15.4	2.71	5.39	5.68	0.360	II	Froth
286D	0.630	0.00183	.0334	64	18.2	3.02	5.39	6.03	0.372	III	Froth
287D	0.630	0.00183	.0407	64	22.2	3.33	5.39	6.66	0.376	III	Ripple
288D	0.630	0.00183	.0308	64	16.8	2.71	5.39	6.20	0.372	II	Froth
289D	0.630	0.00183	.0451	64	24.6	4.49	5.39	5.48	0.388	IV	Film
290D	0.630	0.00183	.0576	64	31.5	4.91	5.39	6.42	0.425	IV	Film
380D	1.025	0.0050	0.0620	69	12.4	2.32	5.45	5.35	0.312	II	Froth
381D	1.025	0.0050	0.117	69	23.4	3.65	5.45	6.41	0.288	III	Froth
382D	1.025	0.0050	0.158	70	31.6	4.34	5.47	7.28	0.293	IV	Ripple
383D	1.025	0.0050	0.137	75	27.4	4.13	5.53	6.63	0.295	III	Ripple
386D	1.025	0.0050	0.0303	73	6.06	2.47	5.51	2.45	0.256	I	Slug
387D	1.025	0.0050	0.0568	74	11.4	2.26	5.51	5.04	0.330	II	Froth
388D	1.025	0.0050	0.0775	72	15.5	2.81	5.51	5.52	0.321	III	Froth
389D	1.025	0.0050	0.0157	73	3.20	1.83	5.51	1.75	0.346	I	Slug
390D	1.025	0.0050	0.0285	72	5.80	2.28	5.51	2.54	0.272	I	Slug
391D	1.025	0.0050	0.0383	73	7.60	2.74	5.51	2.77	0.252	I	Slug
392D	1.025	0.0050	0.00788	70	1.60	0.930	5.47	1.72	0.498	I	Slug
345S	1.50	0.0107	0.396	79	37.2	5.02	5.55	7.41	0.217	III	Ripple
346S	1.50	0.0107	0.214	66	20.1	3.52	5.41	5.71	0.281	III	Froth
350S	1.50	0.0107	0.282	67	26.5	3.97	5.42	6.68	0.244	III	Froth
351S	1.50	0.0107	0.170	67	16.0	2.70	5.42	5.93	0.320	III	Froth
352S	1.50	0.0107	0.128	67	12.0	2.37	5.42	5.06	0.350	III	Froth
353S	1.50	0.0107	0.0898	67	8.43	2.46	5.42	3.42	0.337	II	Froth
354S	1.50	0.0107	0.0321	67	3.01	1.47	5.42	2.05	0.377	I	Slug
355S	1.50	0.0107	0.0587	67	5.51	2.04	5.42	2.70	0.320	I	Slug
356S	1.50	0.0107	0.0197	79	1.84	0.914	5.55	2.01	0.540	I	Slug
257S	1.50	0.0107	0.0493	79	4.63	1.81	5.55	2.56	0.293	I	Slug
258S	1.50	0.0107	0.0888	80	8.34	2.70	5.56	3.09	0.335	II	Froth
259S	1.50	0.0107	0.338	81	31.7	4.94	5.57	6.42	0.241	III	Ripple
360S	1.50	0.0107	0.389	80	36.5	5.15	5.56	7.09	0.232	III	Ripple
481S	2.50	0.0296	0.0586	78	1.98	0.900	5.54	2.20	0.433	I	Slug
482S	2.50	0.0296	0.0731	79	2.48	0.992	5.55	2.50	0.481	I	Slug
483S	2.50	0.0296	0.0940	79	3.20	1.12	5.55	2.85	0.432	I	Slug
484S	2.50	0.0296	0.126	79	4.25	1.25	5.55	3.39	0.377	I	Slug
285S	2.50	0.0296	0.163	78	5.50	1.41	5.54	3.90	0.340	I	Slug
286S	2.50	0.0296	0.199	78	6.74	1.53	5.54	4.41	0.330	I	Slug
487S	2.50	0.0296	0.250	78	8.45	1.74	5.54	4.86	0.340	II	Froth
488S	2.50	0.0296	0.336	78	11.3	1.98	5.54	5.70	0.297	III	Froth
489S	2.50	0.0296	0.295	79	10.0	1.89	5.55	5.30	0.328	III	Frot
490S	2.50	0.0296	0.423	79	14.3	2.22	5.55	6.45	0.277	III	Froth
491S	2.50	0.0296	0.510	78	17.2	2.47	5.54	6.95	0.284	III	Ripple

* At test section temperature and average pressure.
** Column 4 divided by column 3.
***Column 6 divided by column 7.

Interpretation and correlation of results

Effect of diameter on flow pattern

As has previously been shown the flow patterns may best be defined and correlated by reference to the pressure drop regimes which in turn are defined by the two minima and the maximum points in the unit pressure drop-air-water volume ratio curve. The loci of the abscissa values of these points as functions of the superficial water velocity are shown in Figure 19. This figure presents the data for all tube diameters including the data for the 1.025 in. tube reported in Part I. It will be seen that a common locus exists for the first minimum point or that the air-water volume ratio at which the first pressure drop minimum and the transition from Regime I to Regime II occurs is independent of tube diameter. In the cases of the maximum point and the second minimum point, however, the loci depend upon diameter. The locus of the maximum points and that of the second minimum points intersect at an increasing water rate and a decreasing air-water volume ratio as the tube diameter increases. Insufficient data were obtained to completely define the maximum and second minimum loci for the 1.50 and 2.50

in. tubes but the trends are quite well established and are indicated by dashed lines.

These loci lines are further correlated and related to the flow patterns in Figures 20, 21, and 22. Figure 20 shows the single locus of the first minimum points for all four diameters and the flow-pattern transition lines. The bubble-slug transition appears as a single line for all diameters. The slug-froth transition lines are slightly different for each diameter because of the effect of diameter on the locus of the maximum points. The different loci for the maximum points were, by trial, found to be brought closer together by plotting superficial water velocity V_L, vs. $R_V D^{1/3}$ as in Figure 21. The spreading of these loci at high water velocities reflects the effect of water velocity on their mergence with the loci of the second minimum points. On this plot the slug-froth transition again appears as a family of lines, one for each diameter. Figure 22 presents the locus of the second minimum points as functions of V_L vs. $R_V D^{-1/3}$. Again the abscissa was determined by trial to bring the three separate loci lines of Figure 19 into coincidence. The transitions from froth to ripple and from ripple to film flow each appear pretty well as single lines on this plot.

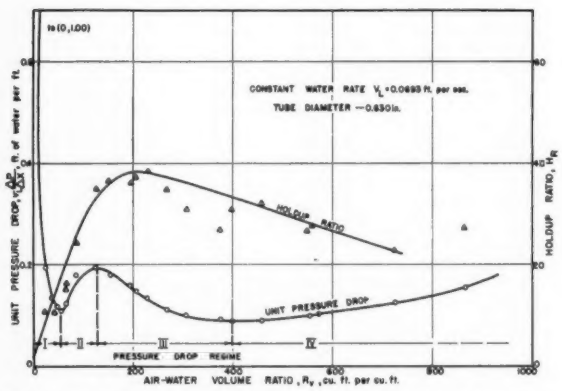

Figure 2—Pressure drop and holdup relationship, D = 0.630 ins., V_L = 0.0693 ft./sec.

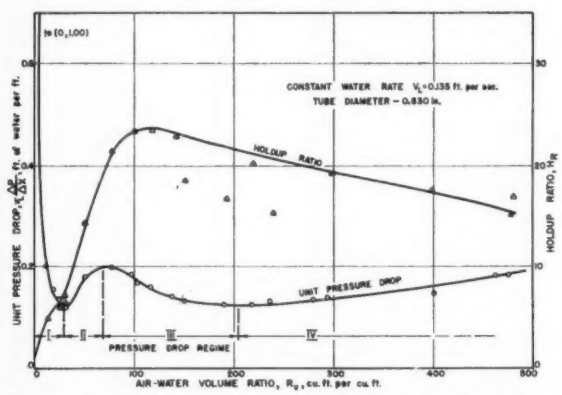

Figure 3—Pressure drop and holdup relationship, D = 0.630 ins., V_L = 0.135 ft./sec.

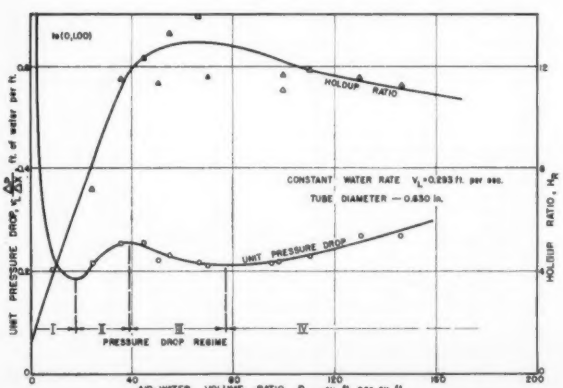

Figure 4—Pressure drop and holdup relationship, D = 0.630 ins., V_L = 0.293 ft./sec.

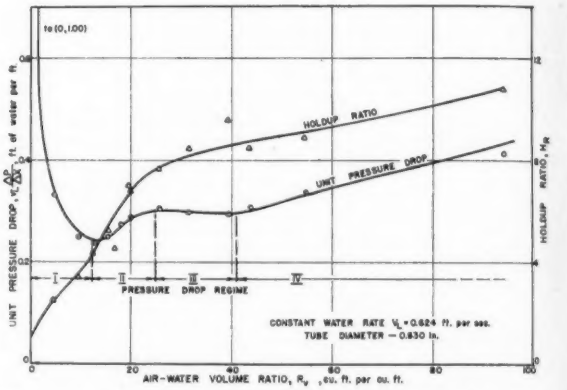

Figure 5—Pressure drop and holdup relationship, D = 0.630 ins., V_L = 0.624 ft./sec.

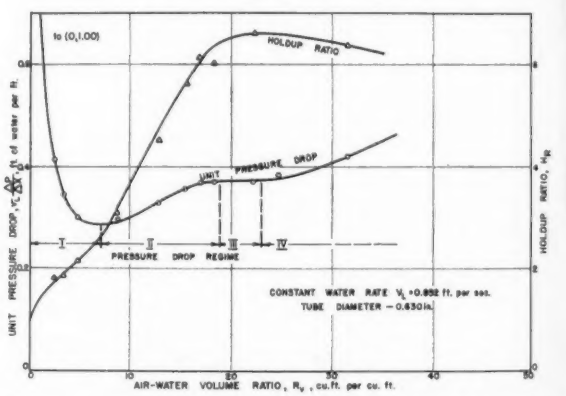

Figure 6—Pressure drop and holdup relationship, D = 0.630 ins., V_L = 0.852 ft./sec.

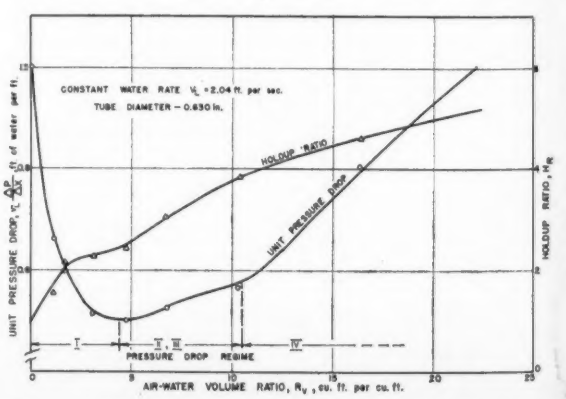

Figure 7—Pressure drop and holdup relationship, D = 0.630 ins., V_L = 2.04 ft./sec.

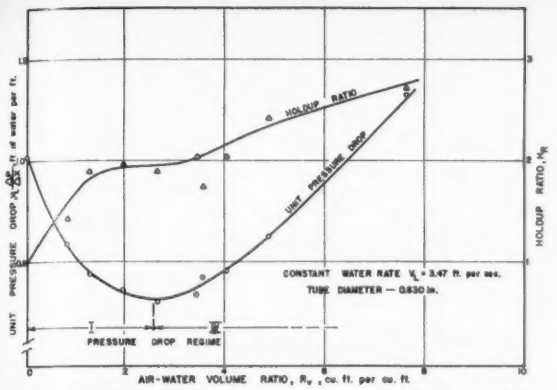

Figure 8—Pressure drop and holdup relationship, D = 0.630 ins., V_L = 3.47 ft./sec.

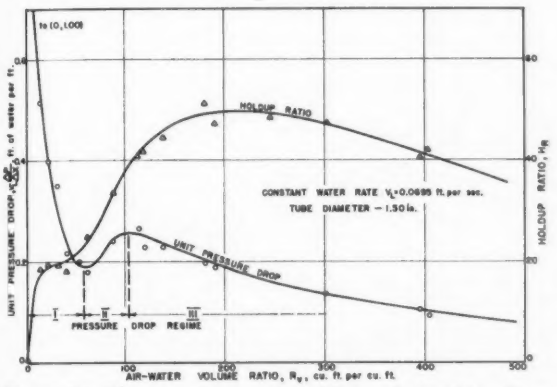

Figure 9—Pressure drop and holdup relationship, D = 1.50 ins., V_L = 0.0695 ft./sec.

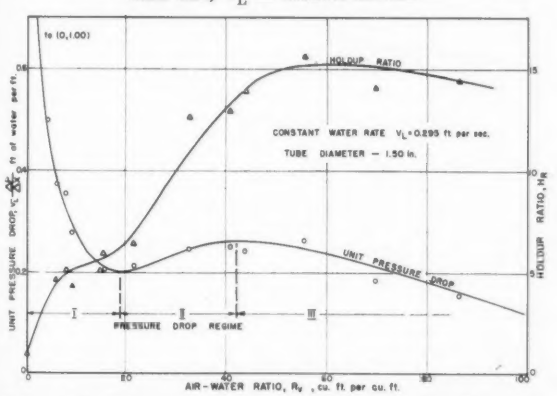

Figure 10—Pressure drop and holdup relationship, D = 1.50 ins., V_L = 0.295 ft./sec.

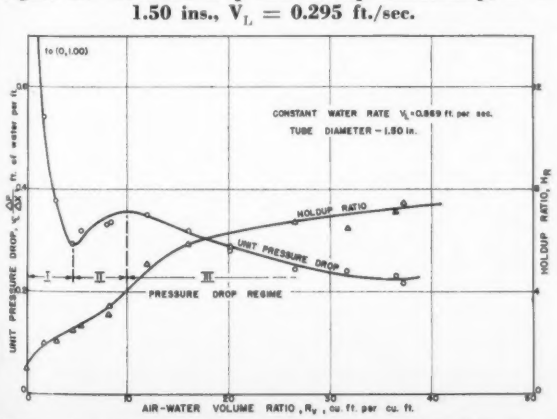

Figure 11—Pressure drop and holdup relationship, D = 1.50 ins., V_L = 0.869 ft./sec.

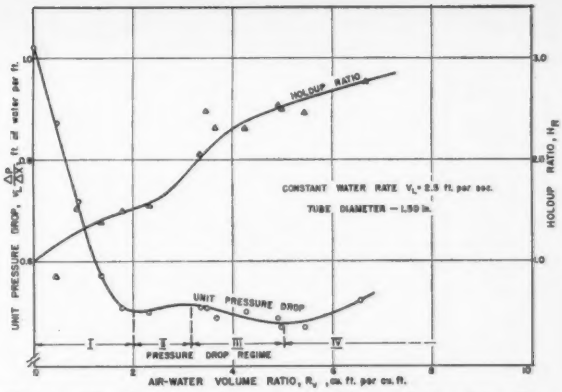

Figure 12—Pressure drop and holdup relationship, D = 1.50 ins., V_L = 2.50 ft./sec.

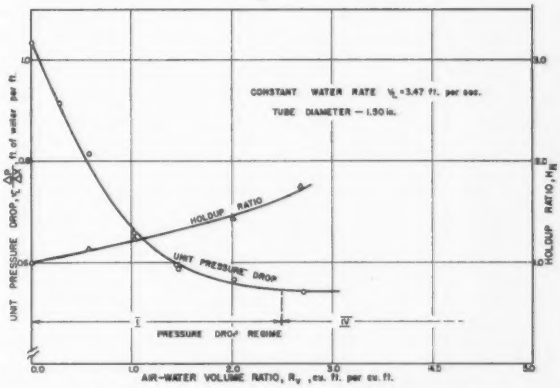

Figure 13—Pressure drop and holdup relationship, D = 1.50 ins., V_L = 3.47 ft./sec.

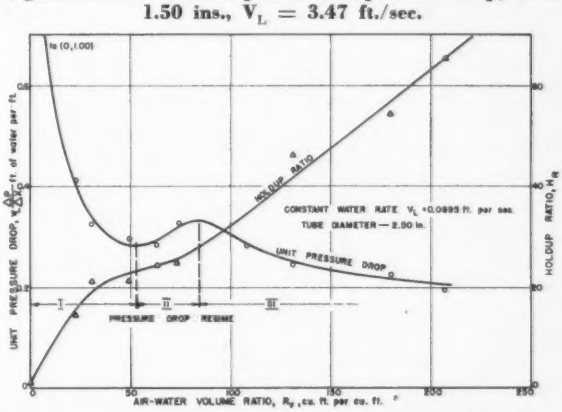

Figure 14—Pressure drop and holdup relationship, D = 2.50 ins., V_L = 0.0695 ft./sec.

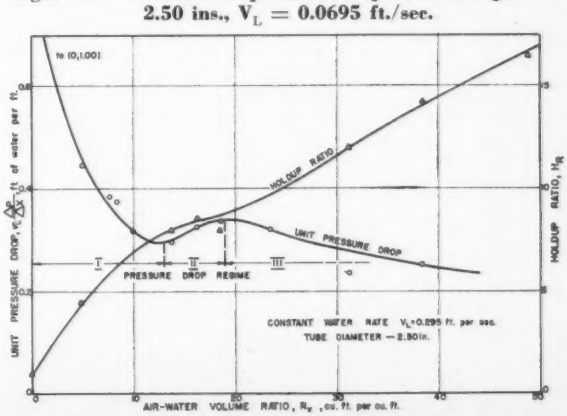

Figure 15—Pressure drop and holdup relationship, D = 2.50 ins., V_L = 0.295 ft./sec.

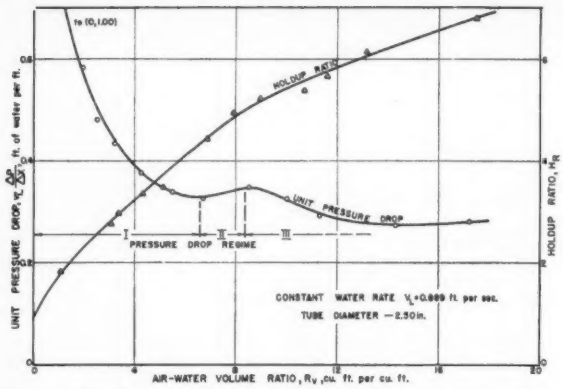

Figure 16—Pressure drop and holdup relationship, D = 2.50 ins., V_L = 0.869 ft./sec.

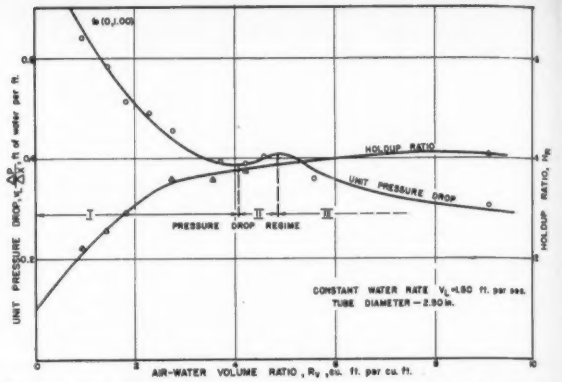

Figure 17—Pressure drop and holdup relationship, D = 2.50 ins., V_L = 1.50 ft./sec.

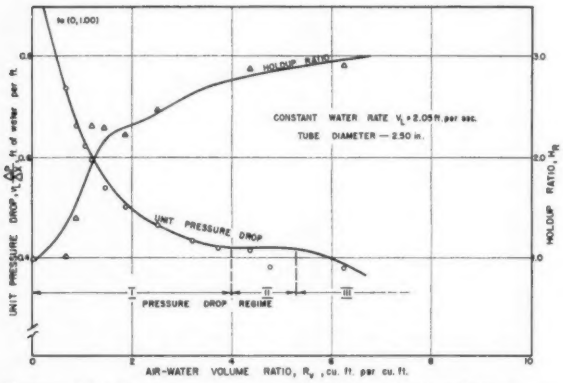

Figure 18—Pressure drop and holdup relationship, D = 2.50 ins., V_L = 2.05 ft./sec.

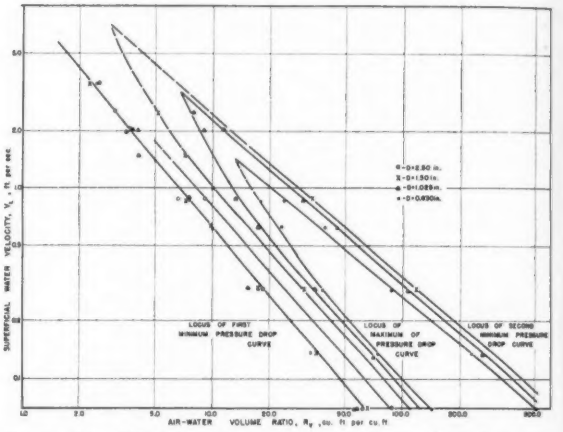

Figure 19—Minima and maximum pressure drop loci (vs. R_V).

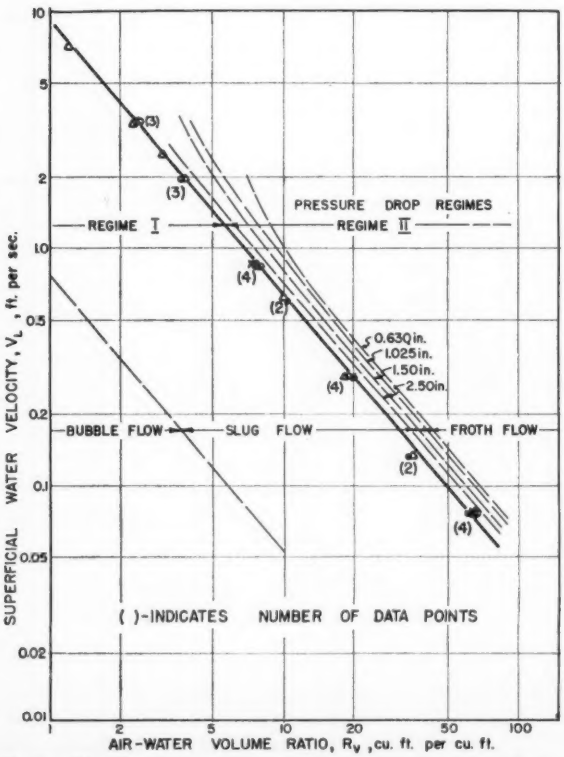

Figure 20—First pressure drop minimum locus (vs. R_V).

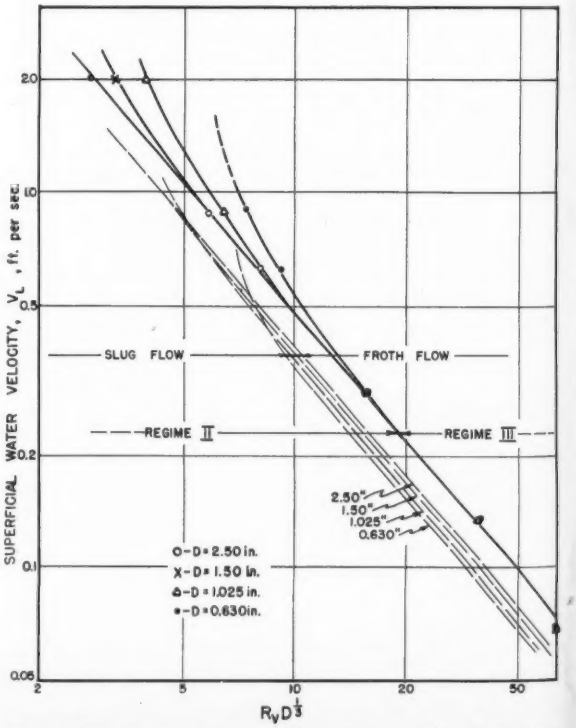

Figure 21—Pressure drop maximum locus (vs. $R_V D^{1/3}$).

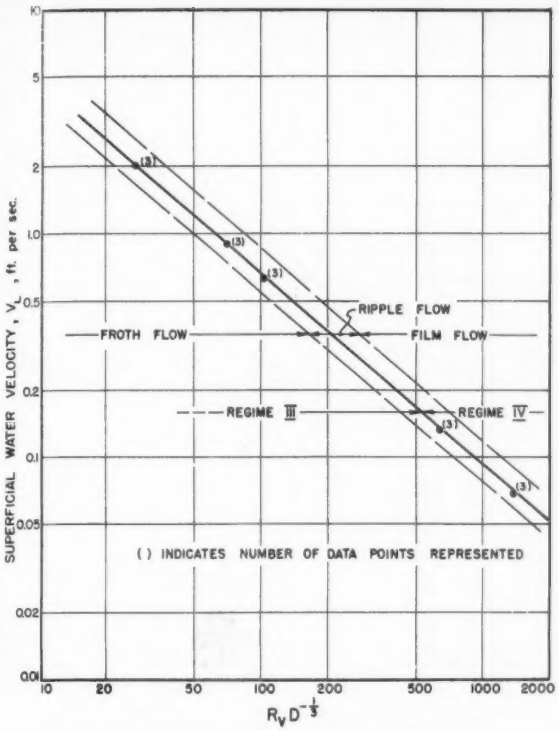

Figure 22—Second pressure drop minimum locus (vs. $R_V D^{-1/3}$).

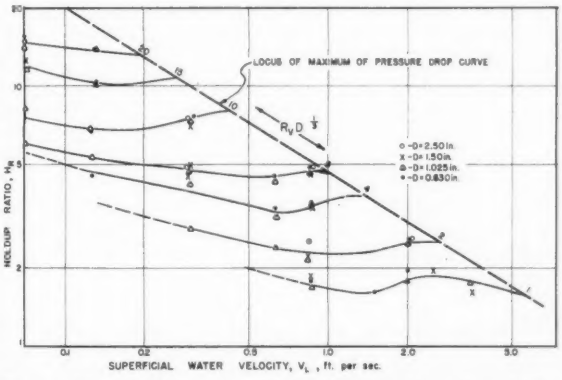

Figure 23—Holdup ratio correlation Regimes I and II.

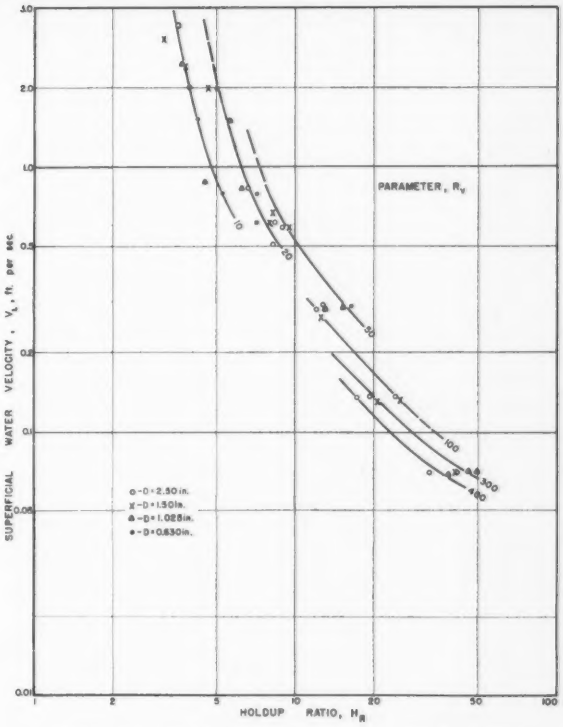

Figure 24—Holdup ratio correlation Regime III.

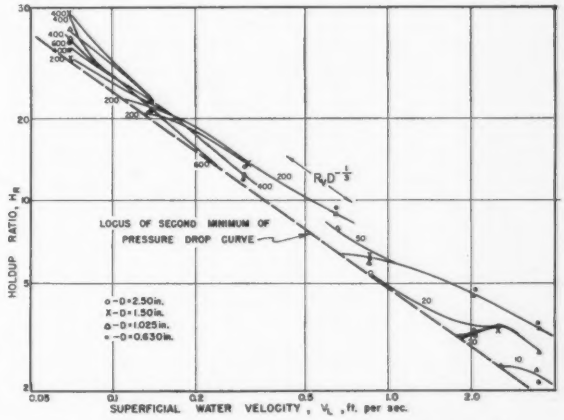

Figure 25—Holdup ratio correlation Regime IV.

Effect of diameter on holdup

The holdup data of Figures 2-18 inclusive and that presented in Part I were cross plotted and analyzed to determine the effect of tube diameter on holdup. By trial it was found that all the holdup data for Regimes I and II could be correlated in terms of the superficial water velocity and the parameter $R_V D^{1/3}$. The correlation is indicated in Figure 23. The data for Regime III correlate well in terms of the parameter R_V alone as shown in Figure 24. The data for Regime IV were found to correlate reasonably well with the parameter $R_V D^{-1/3}$ as illustrated in Figure 25.

Effect of diameter on pressure drop

The total pressure drop was separated into its two components by calculation using Eq. (1). Friction factors were then evaluated from Eq. (2). Numerical values of the pressure drop components and the friction factors are presented in Table 2 deposited as Document No. 5274* with the American Documentation Institute Auxiliary Publication Project, Photo Duplication Service, Library of Congress, Washington 25, D.C. The general nature of the effect of tubing diameter on the friction factor is shown in Figure 26 which presents data for all four diameters at a typical constant water velocity of some

*A more detailed form of this paper has been deposited as Document No. 5724 with the ADI Auxiliary Publications Project, Photoduplication Service, Library of Congress, Washington 25, D.C. A copy may be secured by citing the Document No. and by remitting $1.25 for photoprints, or $1.25 for 35 mm. microfilm. Advance payment is required. Make checks or money orders payable to: Chief, Photoduplication Service, Library of Congress.

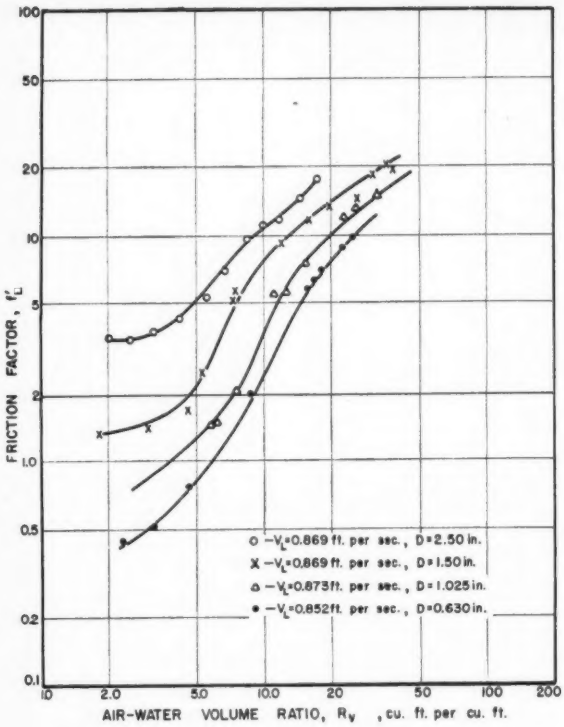

Figure 26—Typical friction factor relationships.

0.87 ft./sec. By trial it was found that a very good correlation was obtained by plotting friction factor vs. DV_L with a parameter of $V_G D^{3.5}$, where V_G is the superficial gas phase velocity based upon the average flowing temperature and pressure and upon the total tube cross section, ft./sec. This is shown in Figure 27. The abscissa DV_L was chosen as representing a reduced form of the superficial Reynolds number for the liquid phase. The parameter $V_G D^{3.5}$ may be considered the product of a reduced form of the superficial Reynolds number based on the gas phase and the term $D^{2.5}$. The conventional single phase friction factor corresponding to a parameter value of zero, is shown for reference purposes. The two phase friction factor curves lie well above and to the right of the single phase line but approach the latter at high abscissa values.

Conclusions

The new data and correlations enable the prediction, for any diameter between, say 0.5 and 3.0 in., of the flow pattern, the holdup and the pressure drop as functions of the diameter and the air and water rates for the upwards vertical flow of air-water mixtures at an average pressure and temperature of 36.0 psia and 70-85°F. respectively. The correlations are restricted in application to systems where the average pressure is constant at 36.0 psia and where the fractional change in specific volume of the water saturated gas phase is small enough to justify the use of an average valve. The effect of average pressure (or gas phase density) is now under study and will be reported upon shortly.

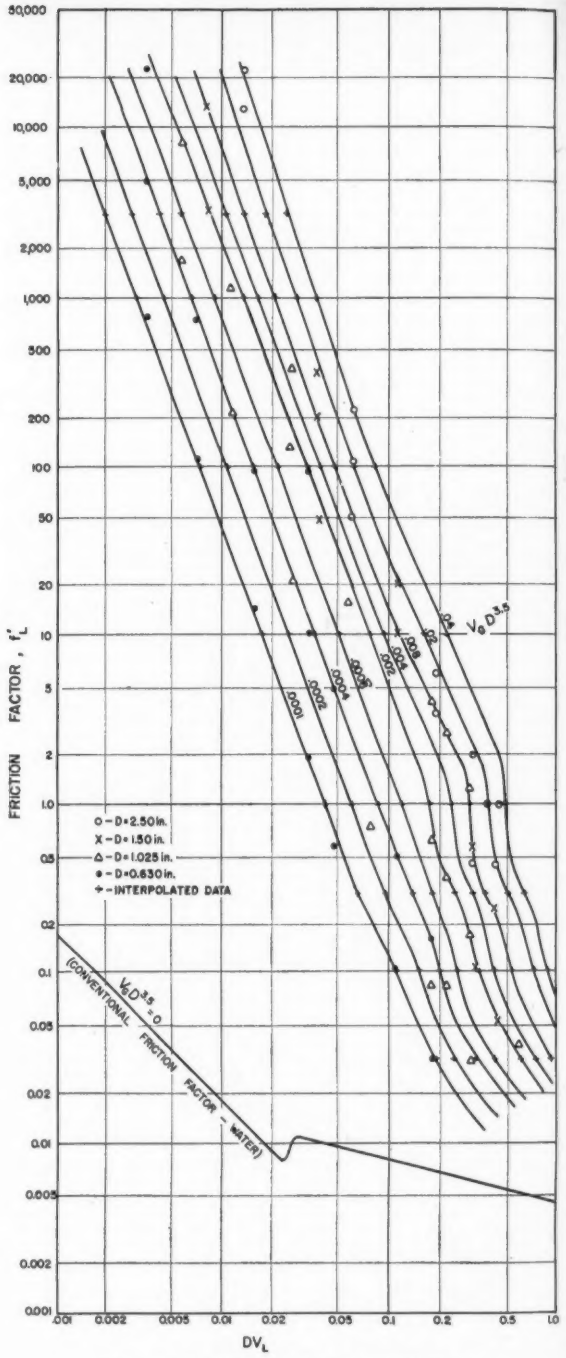

Figure 27—Friction factor correlation.

References

(1) Govier, G. W., Radford, B. A., and Dunn, J. S. C., C.J.Ch.E. 35, 38, 1957.

Acknowledgement

The data reported here are taken from the M.Sc. Thesis of W. L. Short submitted September 30, 1957, to the Department of Chemical and Petroleum Engineering and the Faculty of Graduate Studies of the University of Alberta.

The authors gratefully acknowledge the interest and financial support of Imperial Oil Limited.

* * *

A Heat Exchanger Design for Heavy Water Reactor Service[1]

A. D. DUFF, JR.[2] *and E. E. WILSON*[3]

The volume of heavy water required for a power reactor plant using this moderator has an important influence on investment. Likewise, the cost of leakage justifies extraordinary containment measures. A heat exchanger design is described which satisfies these requirements, as well as those imposed by the radiation field in which the equipment must operate.

Heavy water heat exchangers in the primary coolant loops of a nuclear power plant pose many design problems not encountered in conventional practice. These problems arise from three basic considerations as shown in Table 1. First is the high cost of heavy water, currently quoted by the United States Atomic Energy Commission at $28.00/lb. Second is the radioactivity induced in the heavy water stream. Third is the necessity for maintaining the heavy water at a very high level of isotopic purity in order to maintain its efficacy as a moderator in the reactor.

Table 1

Basic Design Considerations	Nuclear Heavy Water Heat Exchanger
● Cost of Heavy Water — $28/lb.	
● Radioactivity in Heavy Water	
● High Isotopic Purity Requirements	

Owing to the cost of heavy water, the hold-up in the exchangers represents a substantial investment and requires that optimization calculations include the cost, normally neglected for conventional fluids. This materially affects the usual ratio of volume to effective heat transfer surface. Relatively high over-all heat transfer coefficients and friction losses are a natural consequence. The volume contained in connections from the piping system to the heat exchangers again has an important effect on design of heads and connecting piping. The cost of heavy water also requires a high degree of integrity against leakage in the design. For example, a leak rate of 5 drops/min. represents an annual loss of about $10,000.00.

Radioactivity in the heavy water arises from tritium formed by exposure of deuterium to neutrons, from activity induced by neutron bombardment of corrosion products and other trace impurities and from fission products in the event of fuel failure. This condition lends added weight to the need for freedom from leakage, because of the potential hazard to personnel resulting from entry of radioactive heavy water into the secondary loop, for example. Similarly, maintenance of radioactive equipment is both time-consuming and expensive, because of limits on exposure of personnel, the need for protective clothing, and the like. The heat exchanger, therefore, must be so designed as to permit reduction of radioactive levels, by cleaning, to a point where reasonable maintenance work can be done, at intervals, over a relatively long period. This requires that it be possible to decontaminate the equipment without disassembling it and, preferably, without necessitating close contact between maintenance personnel and the equipment. Ideally, the exchanger should be free from places where contaminants can lodge, and should be capable of being decontaminated by some relatively simple technique, such as a high volume flush, with provision, of course, for disposal of the contaminants.

Minimizing the necessity for performing any maintenance work at all is fully as important as simplifying maintenance functions. This is, of course, true in conventional plant design, but, for the reasons stated earlier, assumes far greater proportions for the nuclear case.

The need for maintenance of isotopic purity of the moderator is still another reason for designing against leakage. The entry of secondary coolants, such as light water, into the heavy water stream requires installation and operation of separating equipment, which can represent an appreciable cost.

The factors mentioned so far tend to make the cost of heat transfer surface for the nuclear heavy water exchanger higher than for normal utility or chemical plant service. The achievement of tolerable costs for large units makes it important to use available materials in sizes and specifications reasonably close to normal industrial practice. Similarly, consideration must be given to feasibility of fabrication of exchangers in large units with minimum necessity for developing techniques and skills which depart widely from those employed in the fabricating industry.

As summarized in Table 2, the heavy water heat exchanger in a nuclear plant primary coolant loop must be designed for:

(1) Low heavy water hold-up.
(2) Minimum leakage in either direction.
(3) Minimum maintenance.

[1]*Manuscript received July 23, 1958.*
[2]*Division Engineer, Design Division, Engineering Department, E.I. du Pont de Nemours & Co. Inc., Wilmington, Del.*
[3]*Design Project Manager, Design Division, Engineering Department, E.I. du Pont de Nemours & Co. Inc., Wilmington, Del.*
This article is based on a paper presented at the Joint A.I.Ch.E.-C.I.C. Chemical Engineering Conference in Montreal, April 20-23, 1958.

(4) Ease of required maintenance.
(5) Minimum fabrication cost considering the above requirements.

TABLE 2

DESIGN REQUIREMENTS	NUCLEAR HEAVY WATER HEAT EXCHANGER
• Low Heavy Water Holdup	
• Minimum Leakage in Either Direction	
• Minimum Maintenance	
• Ease of Required Maintenance	
• Minimum Fabrication Cost	

The remainder of this paper will describe how an actual design was developed and executed to meet these requirements, together with comments on fabrication experience and on the ultimate service performance of the equipment. The facilities described were designed for transferring heat from a large flow of heavy water to a light water stream, but the principles involved are applicable to other secondary media.

The parameters of heat load, temperature, and pressure were first determined, after which several alternate basic designs of exchangers were considered. One concept (shown in Figure 1) which may be called the plate type, consisted of sheets of either stainless steel or aluminum, pressed into a multi-channel form. A stack of such sheets would be assembled, and welded or brazed at points of contact. Manifolding arrangements at the ends would permit flow of light water and heavy water through alternate channels. This concept had the advantage of efficient use of material, good heat transfer coefficients on both sides, low cost, low heavy water volume, and probably fairly good decontaminability. Some small experimental units were fabricated and tested, but it was found that necessary fabrication techniques would require considerable development. Furthermore, leak repair, either during fabrication or as a result of failure in service, appeared impractical, and it was judged that the degree of approach to perfection in fabrication technology required to attain zero leakage was beyond any reasonable expectation.

Heat exchangers based on the falling film principle, using either horizontal or vertical tubes, were next considered. Calculations and tests showed, however, that the hold-up for this design was surprisingly high, by comparison with other types. An important factor in holdup for this design was the requirement for dissipating the high inlet velocity which resulted from the use of comparatively small pipe in the main loop.

A number of variations of the shell and tube type of exchanger were then considered. The requirement of low ratio of volume to heat transfer surface favored the smallest practical tube diameter, with heavy water inside the tubes. This led to consideration of $\frac{1}{8}$ in. and $\frac{1}{4}$ in O.D. tubes fastened into tube sheets by rolling, welding, drifting, or combinations of these. Investigation revealed that it was physically possible to expand or weld tubes of these sizes into tube sheet holes. However, the problem of controlling such operations to produce the required tightness of joints, considering the thin tube wall and the delicacy of tools small enough to enter the tubes, made the use of such small tubes unattractive.

An alternate approach (indicated in Figure 2) to the use of these very small tube sizes was suggested by Alco Products Company and consisted of a number of tube ends welded or brazed together into a pack, with a ring welded to the periphery of the pack and a reducing fitting to the ring. The reducer, in turn, would be fastened to a tube sheet by conventional means. Diameters of 1 in. to 2 in. were visualized for that end of the reducer which would be fastened to the tube sheet. It was visualized that the tubes after leaving the end cluster would be splayed out and held in a rectangular pattern by small square tube supports. Experimental assemblies of this type were made and leak-tested. Considerable difficulty was experienced in securing "Freon"-tight joints. The difficulty lay in securing a deep enough joint between adjacent tubes to make an effective seal. A further drawback was that there were no means for correcting leaks after assembly of tubes into the pack. Thus, there would be a substantial amount of heat transfer surface lost if leaks showed up after fabrication, since it would be necessary to plug the entire pack.

Since no practical method of using small tubes had been found, it was concluded that the best approach lay in the use of larger tubes individually fastened to tube sheets, with heavy water volume minimized by placing cores in the tubes. Discussions of the problems were held with manufacturers, who, at first, were inclined to regard $\frac{5}{8}$ in. O.D. tubes as the smallest practical size for this equipment. Numerous calculations and some development work led to the use of $\frac{1}{2}$ in O.D., type 304 stainless steel tubes, with 0.3 in. diameter solid core rods. Double tube sheets were considered essential to permit rapid detection and location of any leakage which might occur, to minimize loss of heavy water into the light water stream, and to collect leakage, thereby permitting longer operation under leakage conditions. Use of maximum length tubes

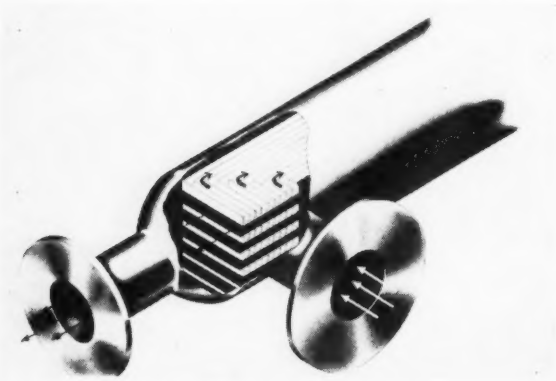

Figure 1—Plate type heat exchanger.

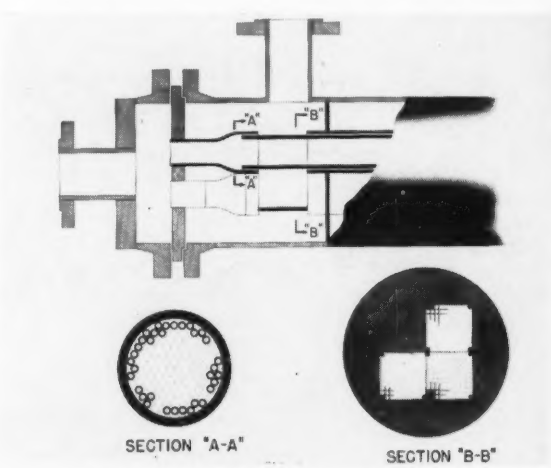

Figure 2—Tube Pack heat exchanger.

was settled upon so as to minimize number of units and joints, thereby reducing cost as well as number of potential sources of maintenance.

One interesting aspect of the heat transfer calculations may be briefly mentioned. Tube side flow was found to lie in the transition region between laminar and well-defined turbulent flow. Because of the unusual ratio of length to diameter, the calculated heat transfer coefficient was found to be somewhat lower than might be expected. Both tube side and shell side coefficient were verified experimentally to minimize allowances for uncertainty.

For the final design, tube size was selected as $\frac{1}{2}$ in. O.D., 18 gage, type 304L stainless steel. Tubes were to be 29 ft. 6 in. long which was the greatest length available from most producers. Design features of the unit, such as number of tubes, core size, baffling, and the like, were established by optimizing calculations described in a paper by Brinn and Cichelli [1].

In carrying out the tube sheet design, it was calculated that a thickness of 7 in. to 9 in. would be required if unstayed sheets were used, because of the large shell diameter. It was soon apparent that the cost and time required for drilling these tube sheets would be intolerable, even if it were assumed that the problem of controlling drift of the drill over this length could be solved. The tube sheets were therefore recalculated using staybolts and a thickness of $1\frac{3}{4}$ in. found adequate. In computing stresses, credit was taken for support of the outer tube sheet by the inner one via the tubes, since the staybolts did not bear on the inner tube sheets, as shown in Figure 5.

The shell (Figure 5) was of conventional cylindrical fixed tube sheet design. Stainless steel plate was used, rather than carbon steel, so as to avoid expansion joints which were believed to be a potential source of maintenance. The shell closure was effected by welding it to the inner tube sheets. Tube supports, cross flow baffles, impingement baffles, and inlet and outlet nozzles were conventional.

The heads were gasketed to the other tube sheet, as shown in Figure 5, by means of rectangular cross section, neoprene gaskets, which were essentially fully confined and compressed by controlled bolting. Consideration was given to using a welded joint, but it was decided that conservative design and meticulous fabrication could produce an essentially maintenance-free gasketed joint. Stay-bolts were threaded into the outer tube sheet and passed through bosses on the heads with nuts on their outer ends which served to transfer the tube sheet load to the head. O-rings on the bodies of the bolts provided a seal. As mentioned previously, the exchanger shell terminated at the inner tube sheet at each end with the space between the two tube sheets, in each case, being closed by a removable shroud.

The head design, shown in Figure 4, is an interesting feature of this heat exchanger and was described in a paper by Cichelli & Boucher [2]. The basic requirements were low volume, low pressure drop, and reasonably equal distribution of fluid to the tubes, in addition to furnishing structural support to the tube sheets. The problem was

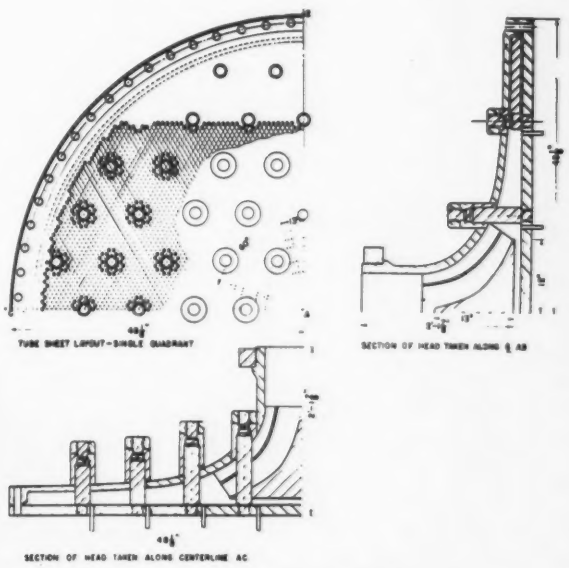

Figure 4—Heat exchanger head details.

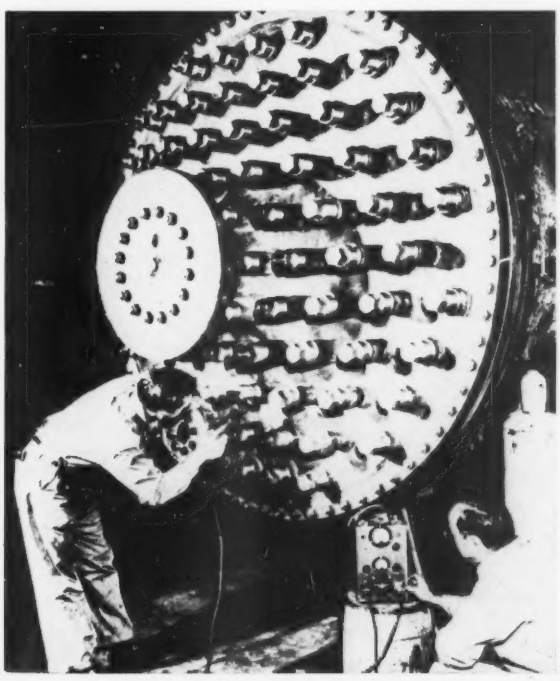

Figure 3—Heat exchanger in place with the inlet nozzle covered for testing.

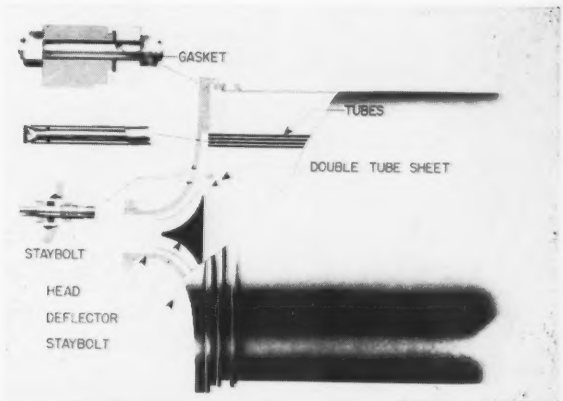

Figure 5—Heavy water heat exchanger.

complicated by the numerous staybolts used for supporting the outer tube sheets, which lie across the water flow path. Figure 3 shows the head in place with the inlet nozzle covered for testing.

Each heat exchanger was supported on a pair of standard railroad car trucks. These facilitated handling within the building and guided the unit as it expanded and contracted in service. In practice, one set of trucks was anchored and the other allowed to float.

Mention was made earlier of the desirability of utilizing established techniques and standard materials. It is worth noting that even though this principle was followed, a substantial portion of the engineering effort required for these heat exchangers was devoted to fabrication and material procurement. Perhaps the largest procurement effort was that of obtaining the necessary tubing in the required quantities. The efforts of several redraw mills were needed to produce the required amounts, and, of course, it was necessary to standardize testing and dimensional control so that tubes from the several mills could be used interchangeably. Seamless, butt-welded, and so-called swaged tubing all were used, and experience was good with all types.

An essential feature of the fabrication phase was exhaustive testing. After each row of tubes was inserted and fastened, tube to tube sheet joints were leak-tested, first with "Freon" and then with hydrostatic pressure. It was found important to make the "Freon" test prior to the hydrostatic test, because it had been demonstrated earlier that water could effectively seal apertures through which the "Freon" would otherwise indicate a leak. The first exchanger was also thermally cycled to simulate operation and uncover any foreseen effects of temperature change.

As a step to minimize eventual contamination of the system in which the heat exchangers were to operate, the units were cleaned by shooting wool felt pellets through the tubes with a compressed air gun. Heads were cleaned separately by conventional methods.

Actual experience with operating these exchangers has been very favorable. Heat transfer coefficients have been found close to predicted values. A few leaks have occurred in service at head gaskets, and staybolts, and in two cases, tubes chafed through on tube supports. However, the number of such faults has been extremely low by any standard. The extreme measures taken to assure freedom from leakage or from the need for maintenance have been profitable. Build-up of activity in these exchangers has occurred, however, with the result that some recent process changes made were relatively costly due to the limitations on exposure of personnel. In designing new exchangers for similar service, even greater attention to details for preventing entrapment of radioactive particles would seem warranted. Development of techniques for the use of small tubes could result in substantial cost reductions.

In conclusion, the authors feel that the initial requirements of low volume, minimum leakage, minimum maintenance, and ability to decontaminate were achieved at a cost which was reasonable in the light of the requirements.

References

(1) Cichelli, M. T., and Brinn, M. S., Chem. Eng. 63, 196 (1956).
(2) Cichelli, M. T., and Boucher, D. F., Chem. Eng. Prgr. 52, 213 (1956).

Acknowledgement

The information contained in this paper was developed during the course of work under Contract AT(07-2)-1 with the United States Atomic Energy Commission whose permission for publication is gratefully acknowledged.

Thanks are also extended to C. C. Lockhart, M. G. Stroud, W. R. Heald, and others for their assistance in the preparation of this paper.

★ ★ ★

First Order Rate Processes and Axial Dispersion in Packed Bed Reactors

JAMES J. CARBERRY[2]

By employing recently secured data for the axial dispersion of mass flowing through fixed beds, it is shown that for first order isothermal processes conducted in fixed beds of practical aspect ratios (L/D_p), the effect of mixing upon kinetics is insignificant. It follows that in shallow bed systems usually employed in kinetic research efforts, the influence of axial mixing cannot be ignored, particularly in the case of a liquid reactant. The dispersion data and the analyses support the contention of Ergun [14] and the recent treatment of the problem by Epstein [16].

THE importance of fixed bed processes in the chemical and allied industries has motivated numerous theoretical and experimental analyses of the distribution of heat and mass in fixed beds. Early attention was given to the problem of radial diffusion of mass by Bernard and Wilhelm [1]. In a recent text, Smith [2] discusses the work of those who concerned themselves with the radial mixing problem.

The attention focused upon the distribution of heat and mass is obviously justified by the simple fact that point reaction rates in a packed bed depend uniquely upon concentrations of heat and mass at a given point. Obviously, the goal of rational reactor design demands a basis whereby these concentration distributions may be predicted. The ingenious design method of Baron [3] illustrates this point emphatically.

Axial dispersion

The problem of radial dispersion having been treated rather thoroughly, that of axial or longitudinal dispersion has only recently attracted attention. Danckwerts [4], Kramers, and Alberda [5], and Carberry and Bretton [6] studied the dispersion of tagged water flowing through fixed beds. McHenry and Wilhelm [7] determined axial diffusivities for gas systems while Carberry and Bretton [6] also studied the axial dispersion of a gas in the Reynolds number region below that considered by McHenry and Wilhelm [7].

The general method of correlation is that of relating the Peclet number, $D_p v/E$, to Reynolds number, $D_p v\rho/\mu$. The data of those investigations cited above are shown in Figure 1, based upon average bed velocity. Discussions of these studies are given elsewhere [7, 8].

The limiting value of the Peclet number for axial dispersion in fixed beds has been theoretically shown to be about two by Aris and Amundson [9], McHenry and Wilhelm [7] and Carberry [10]. If a fixed bed is viewed as a series of mixers, then, as stated by Kramers and Alberda [5] as well as others, the numbers of mixers n is related to the bed length L, fluid velocity v and dispersion coefficient E, by

$$n = Lv/2E \quad \ldots\ldots(1)$$

When perfect mixing prevails in each void cell of length γD_p, where γ is the ratio of void cell length to particle diameter (≤ 1), then $n = L/\gamma D_p$ and

$$1/\gamma D_p = v/2E \text{ or } 2/\gamma = D_p v/E = \text{Peclet} \quad \ldots\ldots(2)$$

This is a condition achieved at high levels of turbulence, corresponding to a void cell mixing efficiency of unity. A model relating cell mixing efficiency to the Peclet number has been presented earlier [10]. The model shows that cell mixing efficiency, ϵ is equal to $(\gamma/2)$Pe.

The limiting value of the Peclet number has been predicted and verified experimentally for a gas system by McHenry and Wilhelm [7] while the date of Carberry and Bretton [6] for water appear to approach this limit at high Reynolds numbers as shown in Figure 1.

Axial dispersion and reaction

Hulburt [11], Danckwerts [4], Wehner and Wilhelm [12] and Yagi [13] have treated mathematically the case of first-order kinetics and axial dispersion. While Wehner and Wilhelm [12] have discussed the subtleties of the boundary conditions, it is agreed that the fraction of material unreacted, f, at the bed exit is related to the dispersion and chemical kinetic variables by the equation [4]

$$f = 4a/[(1+a)^2 \exp(-(Pe'/2)(1-a)) - (1-a)^2 \exp(-(Pe'/2)(1+a)] \quad \ldots\ldots(3a)$$

$$\text{where } a = \sqrt{1 + 4k\theta/Pe'} \quad \ldots\ldots(3b)$$

$k\theta$ = first-order time constant

Pe' = Peclet number in terms of bed length, Lv/E

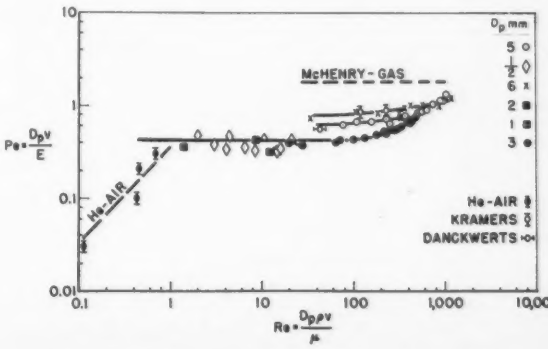

Figure 1—Peclet number vs Reynolds number.

[1]*Manuscript received May 16, 1958.*
[2]*Engineering Research Laboratory, Engineering Department, E.I. du Pont de Nemours & Co. Inc., Wilmington, Delaware. Contribution from the Department of Chemical Engineering, Yale University, New Haven, Conn.*

Since $n = Lv/2E$, then Eq. (3) may be written

$$f_n = 4a/[(1 + a)^2 \exp(-n(1 - a)) - (1 - a)^2 \exp(-n(1 + a))] \quad \ldots\ldots(4a)$$

$$\text{where } a = \sqrt{1 + 2k\theta/n} \quad \ldots\ldots(4b)$$

When piston or plug flow prevails, $n \rightarrow \infty$ and

$$f_\infty = \exp(-k\theta) \quad \ldots\ldots(5)$$

while as $n \rightarrow 1$,

$$f_1 = 1/(1 + k\theta) \quad \ldots\ldots(6)$$

The ratio f_n/f_∞ thus represents the fraction of material unreacted in the effluent of a fixed bed isothermal reactor equivalent dispersionwise to n mixers as compared to the fraction unreacted for a bed of infinite mixers ($E \rightarrow 0$). This ratio is plotted in Figure 2 as a function of $k\theta$ or kL/v. Various levels of conversion for a piston flow reactor are also noted.

Recalling that since

$$n = Lv/2E = (D_p v/E)(L/2D_p) = Pe.L/2D_p \quad \ldots\ldots(7)$$

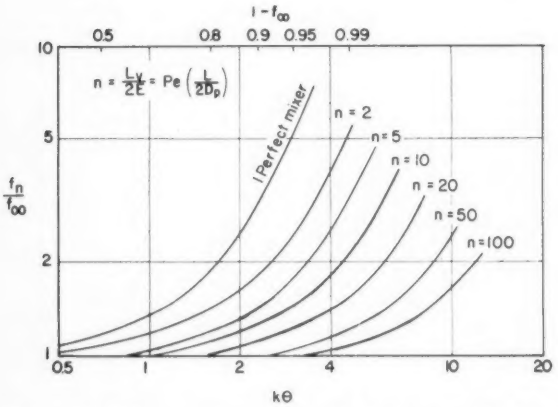

Figure 2—Relative influence of axial mixing upon first-order processes.

and noting the range of Pe values found experimentally and shown in Figure 1, it is immediately apparent that axial dispersion exerts only a trivial effect upon a first order kinetic reaction conducted isothermally in a fixed bed of practical dimensions. This is particularly evident for gaseous systems as the McHenry and Wilhelm data [7] demonstrate that virtually perfect void cell mixing ($Pe \cong 2$) is achieved beyond a Reynolds number value of about 30. While the effect for liquid systems is more pronounced, it is evident that a low value of Pe is not critical so long as the aspect ratio, L/D_p, remains high. Thus the dispersion data and kinetic analysis simply rationalize the common observation that only shallow beds exhibit back-mixing characteristics.

With respect to shallow bed systems, the work of Ergun [14] deserves notice. Analyzing systems employed by laboratory research investigators, i.e., shallow beds and/or differential reactors, Ergun demonstrated that in mass transfer studies, piston flow does not always prevail and in consequence, the use of the log mean driving force to evaluate transfer coefficients is inadmissible. The reader is referred to Ergun's papers [14, 15] for details. Since dispersion data were not available at the time of his analyses, Ergun could only consider the extremes of piston flow and perfect mixing throughout a bed. His point would seem to be deserving of notice insofar as the evidence now at hand would suggest that deviations from piston flow certainly may be critical in experiments carried on in small scale fixed bed reactors where low aspect ratios (L/D_p) are not uncommonly encountered. It is clearly of some significance for an investigator to know whether a given research reactor behaves as 2, 10 or 50 mixers, since rate coefficients can only be accurately derived from a true knowledge of the reactant concentration profile between bed inlet and exit. For example, Epstein [16] did not ignore this point in analyzing mass transfer data secured in shallow beds. He was able to demonstrate, using the idealized model employed by McHenry and Wilhelm [7] to explain their gas dispersion data, that the assumption of piston flow inherent in the usual integration of the mass transfer equation led to transfer coefficients which were only slightly in error for the gas system under study.

Epstein has developed a correction factor, the derivation of which is to be published by him, which permits a modification of the log mean driving force in terms of the number of perfect mixing lengths, L/D_p, characterizing dispersion behavior when $Pe = 2$ and $\gamma = 1$. This relation is of obvious generality since for any value of the Peclet number the number of equivalent mixers n equals $(L/D_p)\epsilon$ or $Lv/2E$. Defining R as the ratio of inlet to outlet driving forces, Epstein's correction factor is [16],

$$Y = \ln R/n(R^{1/n} - 1) \quad \ldots\ldots(8)$$

The use of this relationship with the data of Figure 1 should prove to be a useful guide to those concerned with the procurement of accurate rate coefficients in laboratory scale fixed bed systems.

For the gas mass transfer system considered by Epstein, it was shown, for $R = 8$ and $n = 8$, that Y equalled 0.88. This value of n corresponds to a Pe value of 2 in Epstein's gas system. For a liquid system at the same Reynolds number, the value of Pe would be about 0.5; equivalent to $n = 2$. With the same driving force ratio, R, the correction factor becomes 0.57. Thus the value of the transfer coefficient differs by 75% from that calculated by neglecting dispersion in a liquid mass transfer system for the same driving force ratio.

The contentions of Ergun [15] on mixing in fixed beds appear worthy of notice with respect to liquid systems while Epstein's analysis [16] of gas-solid networks at Reynolds numbers greater than 30 is supported by the dispersion data.

At extremely low values of the Reynolds number for gases (<1) the data of Carberry and Bretton [6] shown in Figure 1 suggest that the axial dispersion coefficient is indeed equal to the molecular diffusivity of the gas system. In consequence, the Peclet number decreases linearly with decrease in Reynolds number in this region of flow. Research studies conducted therein will certainly demand consideration of the dispersion effects upon the rate process under study.

No doubt one could re-examine the research literature and find numerous instances where a serious mixing problem has been ignored in evaluating rate constants and/or j factors. It suffices to cite the work of Gamson, Thodos and Hougen [17] who studied the rate of evaporation of water from pellets in an air stream. Bed depths not exceeding 2½ in. were used for particle sizes up to ¾ in. It is obvious from this discussion that at best, only about three mixing stages prevailed in the study with the largest particle size. Resnick and White [18] studied mass transfer in fixed beds of ½ in. depth. Aspect ratios of about 12 were encountered in their system, however, very low values of the Reynolds number were involved. Since the systems studied comprised naphthalene in air, CO_2 and H_2 respectively, the actual Peclet numbers characterizing the

systems may well have been in the transition region between perfect cell mixing and that dictated by molecular diffusivity. Indeed Resnick and White [18] report an inexplicable effect of particle diameter. As we have seen, for a given bed depth, particle diameter determines the dispersion behavior of the system.

A final point of some importance is that of entrance effects in shallow beds. The author [8] found that for a given Reynolds number the dispersion coefficient, E, increased significantly as bed length is reduced to 6 in., an event anticipated by Ergun [14] some time ago. This anomaly is attributed to acceleration effects as the fluid passes from an unpacked section into the bed. These data merely emphasize the importance of situating dummy beds immediately upstream of an active bed in any shallow bed research work.

Conclusions

In the light of recently correlated axial dispersion data for fixed beds, it is evident that for first order isothermal processes carried out in packed beds of practical aspect (L/D_p) ratios, the effect of axial mixing on the kinetics is negligible.

On the other hand, in bench scale studies in fixed bed reactors, often characterized by low aspect ratios, caution must be exercised in the evaluation of transfer or rate coefficients since the assumption of piston flow may not be justified for liquid systems. As shown by Epstein [16], the mass transfer equation based upon piston flow behavior can be applied, even at low aspect ratios, to a gas system where each void cell acts as a perfect mixer (Pe = 2), provided that a suitable correction factor is applied to the log mean driving force. At low values of the Reynolds number shallow bed experiments in gas or liquid systems demand a consideration of axial mixing as it affects concentration gradients within the system.

Nomenclature

a	= function defined by equations 3b and 4b
D_p	= particle diameter, cm.
E	= axial dispersion coefficient, cm.^{2}/sec.
f	= fraction of reactant remaining at bed exit
k	= first-order rate constant, sec.$^{-1}$
ln	= natural log
L	= bed length, cm.
n	= number of perfect mixing lengths, defined by equation 1
Pe′	= Peclet number in terms of bed length
Pe	= Peclet number in terms of particle diameter
R	= ratio of inlet to outlet driving force as defined by Epstein [16] in equation 8
v	= average fluid velocity in fixed bed
Y	= log mean driving force correction factor [16], equation 8
exp	= exponential, e
θ	= nominal holding time, L/v, sec.
γ	= ratio of void cell length to particle diameter
ϵ	= void cell mixing efficiency

Subscripts

1	= one mixer
n	= n mixers
∞	= infinite number of mixers

References

(1) Bernard, R. A., and Wilhelm, R. H., Chem. Eng. Progr. 46, 233, (1950).
(2) Smith, J. M., Chemical Engineering Kinetics, McGraw-Hill Book Co., Inc., N.Y. (1956).
(3) Baron, T., Chem. Eng. Progr. 48, 118, (1952).
(4) Danckwerts, P. V., Chem. Eng. Sci. 2, 1, (1953).
(5) Kramers, H., and Alberda, G., Chem. Eng. Sci. 2, 173, (1953).
(6) Carberry, J. J., and Bretton, R. H., A.I.Ch.E. Journal 4, No. 3, Sept. (1958). Presented at Chicago A.I.Ch.E. Meeting, Dec., 1957.
(7) McHenry, K. W., and Wilhelm, R. H., A.I.Ch.E. Journal 3, No. 1, 83, (1957).
(8) Carberry, J. J., Doctorate Dissertation, Yale University (1957).
(9) Aris, R., and Amundson, N. R., A.I.Ch.E. Journal, June, 1957.
(10) Carberry, J. J., A.I.Ch.E. Journal 4, No. 1, 13M, (1958).
(11) Hulburt, H. M., Ind. Eng. Chem. 36, 1012, (1944).
(12) Wehner, J. F., and Wilhelm, R. H., Chem. Eng. Sci. 6, 89, (1956).
(13) Yagi, S., et al, Chem. Eng. (Japan) 19, 507, (1955).
(14) Ergun, S., Chem. Eng. Progr. 48, 227, (1952).
(15) Ergun, S., loc. cit., 48, 89, (1952).
(16) Epstein, N., et al., C.J.Ch.E. 35, No. 4, 139, (1957).
(17) Gamson, B. W., Thodos, G., and Hougen, O. A., Trans. A.I.Ch.E. 39, 1, 1943).
(18) Resnick, W., and White, R. R., Chem. Eng. Progr. 45, 377, (1949).

* * *

Correction Factor for Axial Mixing in Packed Beds[1]

NORMAN EPSTEIN[2]

Based on the model of a fixed bed as a series of perfect mixers, a factor is derived for correcting the logarithmic mean driving potentials in the conventional plug-flow equations for fluid-particle heat and mass transfer in packed beds. This factor, which accounts for axial mixing and is a measure of the transfer efficiency of the bed relative to the idealized case where axial mixing is absent, increases towards unity with bed height but decreases with ratio of terminal driving potentials.

RECENT experimental studies [1, 2, 3, 4] on axial mixing in fixed beds have been rationalized by viewing a fixed bed as a number of perfect mixers in series [2, 3, 5, 6]. According to this model, the number of perfect mixers in a fixed bed is given by

$$n = \frac{LV}{2E} = \frac{L}{D_p} \cdot \frac{Pe}{2} \quad \ldots\ldots(1)$$

The axial Peclet number Pe has experimentally [3] and theoretically [3, 5, 6] been found to reach a limiting value of about two for turbulent gas flow through a bed of spheres. For other cases, values smaller than two have been obtained [1, 2, 4]. The number of perfect mixers in a packed bed is thus equal to or less than the number of packing layers L/D_p.

For either heat transfer or mass transfer between a fluid stream and a packing surface maintained at uniform temperature and/or concentration, the assumption of no longitudinal mixing leads to the conventional integrated rate equations containing the logarithmic mean of terminal driving potentials. The actual presence of axial mixing in a packed bed precludes the use of these plug-flow equations, unless a suitable correction factor F is employed to modify the log mean driving potential. Such a factor would be analagous to those used to modify LMTD in multi-pass shell-and-tube heat exchangers [7]. The modified equations would then appear as

$$q = hA\,(\Delta t)_{lm}F \quad \ldots\ldots(2)$$

for heat transfer, and

$$N = k_y A\,(\Delta Y)_{lm}F \quad \ldots\ldots(3)$$

for mass transfer. The derivation of an expression for F follows.

Derivation

Consider a fluid entering a packed bed at temperature t_o, transferring heat to the particle surface which is maintained at uniform temperature t^*, and leaving the bed at temperature t_n. Such would be the case, for example, in a fixed bed of particles undergoing gas drying within the constant rate period [8]. If the bed is viewed as a series of n perfect mixing cells each having surface area A/n and constant heat transfer coefficient h, then for the first mixing cell, steady state heat transfer results in

$$WCp\,(t_o - t_1) = h\,(A/n)\,(t_1 - t^*) \quad \ldots\ldots(4)$$

Rearranging Eq. (4),

$$t_1 = \frac{t_o + Pt^*}{1 + P} \quad \ldots\ldots(4a)$$

or

$$\frac{t_o - t^*}{t_1 - t^*} = 1 + P \quad \ldots\ldots(4b)$$

where

$$P = \frac{hA}{WC_p n} \quad \ldots\ldots(5)$$

Similarly for the second cell,

$$t_2 = \frac{t_1 + Pt^*}{1 + P} \quad \ldots\ldots(6)$$

Combining Eq. (6) and (4a),

$$t_2 = \frac{t_o + 2Pt^* + P^2t^*}{(1 + P)^2} \quad \ldots\ldots(7)$$

or

$$\frac{t_o - t^*}{t_2 - t^*} = (1 + P)^2 \quad \ldots\ldots(7a)$$

Similarly for the third cell,

$$t_3 = \frac{t_2 + Pt^*}{1 + P} \quad \ldots\ldots(8)$$

Combining Eq. (7) and (8),

$$t_3 = \frac{t_o + 3Pt^* + 3P^2t^* + P^3t^*}{(1 + P)^3} \quad \ldots\ldots(9)$$

or

$$\frac{t_o - t^*}{t_3 - t^*} = (1 + P)^3 \quad \ldots\ldots(9a)$$

This pattern continues to the nth mixer, resulting in

$$\frac{t_o - t^*}{t_n - t^*} = (1 + P)^n \quad \ldots\ldots(10)$$

that is

$$R = (1 + P)^n \quad \ldots\ldots(10a)$$

or

$$P = R^{1/n} - 1 \quad \ldots\ldots(10b)$$

An overall heat balance on the packed bed yields

$$q = WC_p\,(t_o - t_n) \quad \ldots\ldots(11)$$

[1]*Manuscript received August 7, 1958.*
[2]*Associate Professor, Department of Chemical Engineering, The University of British Columbia, Vancouver, B.C.*
Contribution from the Department of Chemical Engineering, The University of British Columbia, Vancouver, B.C.

Combining Eq. (11), (2) and (5),

$$F = \frac{t_o - t_n}{(\Delta t)_{lm}} \cdot \frac{1}{nP} \quad \ldots\ldots(12)$$

But for uniform surface temperature t^*,

$$(\Delta t)_{lm} = \frac{(t_o - t^*) - (t_n - t^*)}{\ln \dfrac{t_o - t^*}{t_n - t^*}} = \frac{t_o - t_n}{\ln R} \quad \ldots\ldots(13)$$

Therefore Eq. (12) is equivalent to

$$F = \frac{\ln R}{nP} \quad \ldots\ldots(14)$$

Combining Eq. (14) and (10b),

$$F = \frac{\ln R}{n\,(R^{1/n} - 1)} \quad \ldots\ldots(15)$$

Eq. (15) can be used in conjunction with Eq. (2) and (11) to predict integral heat transfer rates in a packed bed.

The derivation of F for mass transfer follows exactly analagous lines to that for heat transfer and again yields Eq. (15), where R in this case is defined as the ratio $(Y^* - Y_o)/(Y^* - Y_n)$. The mass balance analagous to Eq. (11) is

$$N = G\,(Y_n - Y_o) \quad \ldots\ldots(16)$$

Eq. (15) and (16) can be used in conjunction with Eq. (3) to predict integral mass transfer rates in a packed bed.

Discussion

The axial mixing factor F may be considered a measure of the heat or mass transfer efficiency of a packed bed, being unity in the absence of back-mixing. It has already

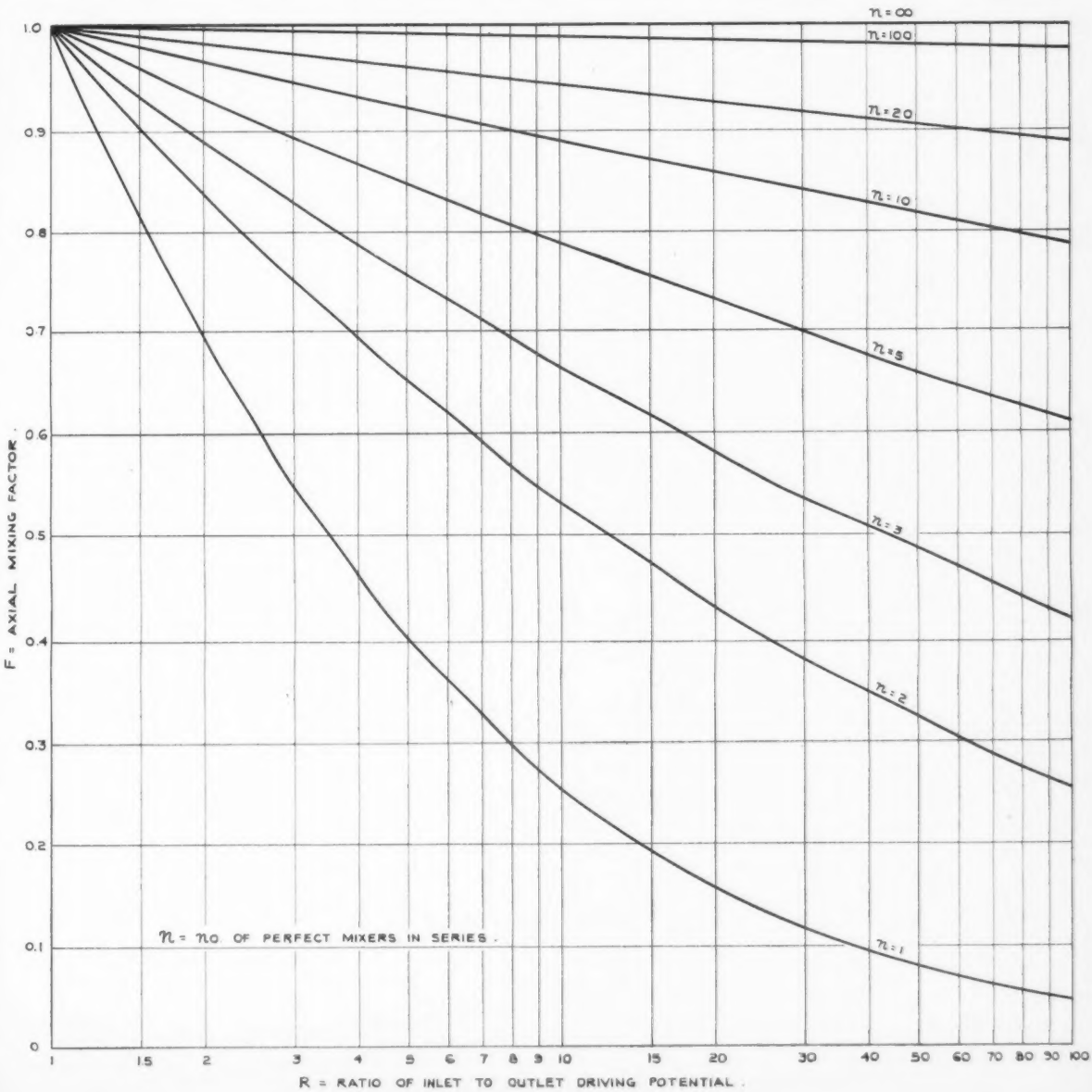

Figure 1—Graphical representation of Equation 15.

been applied by the author in a previous paper [8]. Though rigorously Eq. (15) applies only where t^* or Y^* is uniform throughout the packing, it will probably give a reasonably good answer in Eq. (2) or (3) for many cases of non-uniform surface conditions, especially if a judicious average value is used to represent the surface condition.

Figure 1 is a plot of Eq. (15). It is seen that where the number of perfect mixers is small, that is, for short packed beds, axial mixing markedly reduces the transfer efficiency of the bed. This is particularly true if the longitudinal temperature or concentration change of the fluid is large, resulting in a high value of driving potential ratio R. In addition, end effects in shallow beds probably increase the axial diffusivity, thereby decreasing n according to Eq. (1), and hence the efficiency of transfer is further decreased. The limiting case is that where n = 1, in which the entire bed acts as a perfect mixer.

On the other hand, for deep beds, where n is large, axial mixing can usually be neglected in determining integral transfer rates. The limiting case here is an infinitely long bed, for which F = 1.0.

Mitigating against both extremities is the fact that, in practice, a shallow bed is usually accompanied by a low potential drop and therefore low value of R, while a deep bed is usually accompanied by a high value of R.

Due to neglect of F in Eq. (2) and (3), many reported values in the literature of particle-fluid space-average heat and mass transfer coefficients for packed beds are probably low, especially where shallow beds have been used. Discrepancies between results of various investigations are probably in many cases also caused by this neglect. An attempt to reconcile some of these discrepancies by means of Eq. (1), (2), (3) and (15) is currently being undertaken by the author. This is being supplemented by experiments on very shallow beds.

Nomenclature

A = surface area of packing, sq. ft.
C_p = heat capacity of fluid at constant pressure, B.t.u./(lb.) (°F.)
D_p = particle diameter, ft.
E = axial diffusivity, sq. ft./hr.
F = axial mixing factor, dimensionless
G = flow rate of non-diffusing fluid, lb.-moles/hr.
h = particle-fluid heat transfer coefficient, B.t.u./(hr.) (sq. ft.) (°F.)
k_y = particle-fluid mass transfer coefficient, lb.-moles diffusing component/(hr.) (sq. ft.) (ΔY)
L = depth of packing, ft.
n = number of perfect mixing cells in series, dimensionless
N = mass transfer rate of diffusing component, lb.-moles/hr.
P = hA/WC_pn for heat transfer, dimensionless
= k_yA/Gn for mass transfer, dimensionless
Pe = axial Peclet number = D_pV/E, dimensionless
q = heat transfer rate, B.t.u./hr.
R = ratio of inlet to outlet driving potential: $(t_o - t^*)/(t_n - t^*)$ for heat transfer, $(Y^* - Y_o)/(Y^* - Y_n)$ for mass transfer, dimensionless
t = temperature of fluid stream, °F.
t^* = surface temperature of packing, °F.
Δt = $t - t^*$, °F.
V = interstitial fluid velocity, ft./hr.
W = weight rate of fluid flow, lb./hr.
Y = molal ratio of fluid stream, lb.-moles diffusing component/lb'-mole non-diffusing fluid
Y^* = molal ratio at packing surface, lb.-moles diffusing component/lb.-mole
ΔY = $Y^* - Y$, lb. moles diffusing component/lb.-mole non-diffusing fluid

Subscripts

O = packed bed entrance
1, 2, 3,. . . .n 1st, 2nd, 3rd,. . . .nth perfect mixer
lm = logarithmic mean of terminal conditions

References

(1) Danckwerts, P. V., Chem. Eng. Sci., 2, 1, (1953).
(2) Kramers, H., and Alberda, G., Chem. Eng. Sci., 2, 173, (1953).
(3) McHenry, K. W., Jr., and Wilhelm, R. H., A.I.Ch.E. Journal, 3, 83, (1957).
(4) Carberry, J. J., and Bretton, R. H., "Axial Dispersion of Mass in Flow Through Fixed Beds", presented at Chicago A.I.Ch.E. Meeting, December 9, 1957; A.I.Ch.E. Journal, in press.
(5) Aris, R., and Amundson, N. R., A.I.Ch.E. Journal, 3, 280, (1957).
(6) Carberry, J., A.I.Ch.E. Journal, 4, 13M, (1958).
(7) McAdams, W. H., "Heat Transmission", 3rd ed., p. 194, McGraw-Hill, New York, 1954.
(8) Galloway, L. R., Komarnicky, W., and Epstein, N., C.J.Ch.E., 35, 139, (1957).

Acknowledgments

The author is indebted to the National Research Council of Canada and to the U.B.C. President's Committee on Research for their continuing financial support of studies in momentum, heat and mass transfer. Thanks are also due to the U.B.C. Computing Centre for programming Eq. (15) on an Alwac computer.

★ ★ ★

Some Procedures for the Evaluation of Reactor Fuels and Sheathing Materials at Chalk River[1]

R. F. S. ROBERTSON[2]

In a power reactor the fuel will be operating under very severe conditions. Consequently before a fuel element can be designed it must be tested under conditions which are similar to those in the reactor, and the effect of a large number of variables on the behavior of the fuel must be investigated.

This paper discusses the fuel development program at Chalk River with special reference to the testing of uranium oxide reactor fuels in loops inserted in the NRX reactor. In these loops water may be recirculated over the test elements at temperatures up to 550°F. and pressures up to 2000 psi. The characteristics of a loop are described and the results of various tests are briefly discussed.

The testing of sheathing materials such as Zircaloy-2 and aluminum-nickel alloys is also described.

THE main objective, towards which most work at Chalk River is directed, is the production of economic nuclear power. There are many routes to this objective, some apparently more promising than others, and the one which Atomic Energy of Canada Limited has chosen is the use of natural uranium dioxide as the fuel and heavy water as moderator and coolant.

This paper does not pretend to be in any way a presentation of technical data, but rather is a general discussion of the program to examine the irradiation behavior of reactor fuels and sheathing materials which is now underway at Chalk River. At the end of the paper will be found a list of recent AECL publications which give more technical details.

Figure 1 shows a schematic representation of the proposed reactor NPD-2 which is being built in conjunction with the Canadian General Electric Co. Limited and Hydro Electric Power Company of Ontario. It can be seen that in essence there are two separate heavy water circuits—a high and a low temperature circuit. The high temperature and pressure circuit is one in which the coolant (D_2O) is recirculated past the fuel which is in the form of UO_2 rods sheathed in Zircaloy-2, a corrosion resistant alloy of zirconium and tin. The fuel is held in roughly 130 channels, each channel consisting of a tube made of Zircaloy-2, which is capable of constraining the high pressures at the temperatures involved. The heat which the heavy water picks up from the fuel is removed in the heat exchangers where water (H_2O) is boiled and the resultant steam is passed to the turbines. The cooled D_2O returns from the heat exchanger to the pumps and thence back to the reactor.

[1]*Manuscript received July 25, 1958.*
[2]*Senior Research Officer, Chemistry and Metallurgy Division, Atomic Energy of Canada Limited. Chalk River, Ont.—presently on loan to Argonne National Laboratories, Lemont, Ill.*
This article is based on a paper presented at the Joint A.I.Ch.E.-C.I.C. Chemical Engineering Conference, Montreal, April 20-23, 1958.

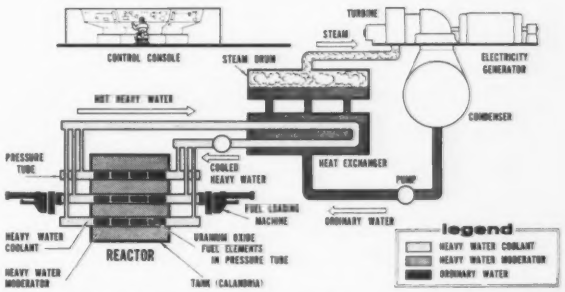

Figure 1—Schematic representation of proposed NPD-2 power reactor.

The second, low temperature and pressure circuit is known as the moderator system. The D_2O is held in a large aluminum vessel which surrounds the pressure tubes. It is maintained at a relatively low temperature (about 120°F.) by circulation through heat exchangers. This system, although it has its own special problems, will not be discussed in this paper which will deal only with the problems associated with the high temperature circuit. The discussion will be further limited to the problems associated with the fuel and sheath. Allison [1] discusses some of the problems associated with the interaction of the high temperature coolant with the rest of the system.

Table 1 gives some information on the NPD-2 reactor, the fuel and some of the conditions under which it will be operating.

TABLE 1

MATERIALS AND OPERATING CONDITIONS FOR A POWER REACTOR

Materials	
Fuel Material	UO_2
Density	10 g/cc (92% theoretical)
Sheath	Zircaloy-2
Pressure Tubes	Zircaloy-2
Other materials in high temp. circuit	Stainless steel, carbon steel, Inconel
Operating Conditions	
Thermal Power	80,000 kw
Electrical Power	20,000 kw
Pressure	1,000 psi
D_2O Temperatures	
Entering Reactor	485°F.
Leaving Reactor	530°F.
Heat flux (fuel surface to water)	135,000 (BTU) (hr^{-1}) (ft^{-2})
Thermal Neutron Flux	5×10^{13} (n) (cm^{-2}) (sec^{-1})

It is quite apparent that the fuel in NPD-2 and in any similar power reactor, will be operating under quite stringent conditions, and moreover under conditions regarding which there is but little experience. Thus it would be a waste of time to design, and unwise to build such a reactor before information was available regarding the behavior of the fuel elements under conditions as nearly as possible those expected in the reactor.

To this end an extensive testing program is proceeding at Chalk River and experiments are being conducted both out of the reactor and in the reactor. This paper will discuss only in-reactor experiments.

Experimental loops

Several test facilities, known as "Loops" have been inserted in the NRX reactor at Chalk River. Westinghouse Atomic Power Division, Pittsburgh, U.S.A. have been responsible for the insertion of the original high temperature and pressure loops in NRX and these loops have been operated in close cooperation with them. A schematic representation of a typical loop is shown in Figures 2 and 3. It can be seen that a loop is really a small version of the primary coolant circuit of a power reactor and in some ways can be looked on as a pilot plant.

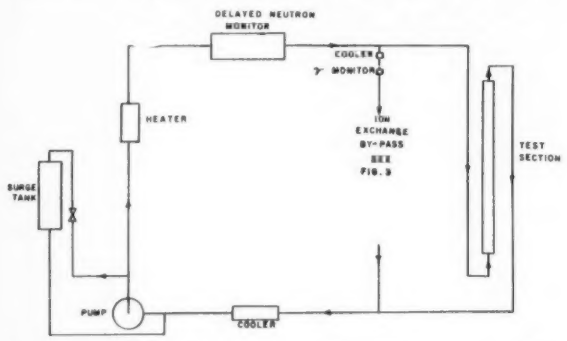

Figure 2 — Schematic diagram of Loop X-2 in the NRX reactor.

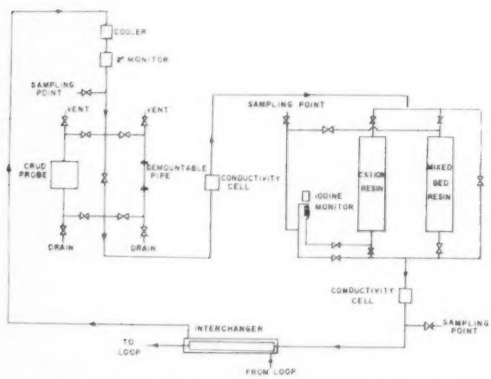

Figure 3—Ion exchange by-pass in Loop X-2.

One of the uranium rods is removed from the NRX reactor and in its place a stainless steel tube is inserted. The fuel under test can be inserted in and removed from this tube through the closure at the top. The coolant, water in most cases, is brought in through the bottom and led out near the top. It is recirculated by the canned rotor pump and is heated electrically to a temperature of 500-550°F. by the heater. Thus there are two possible sources of heat, the heater and the heat produced in the test specimens themselves. Temperatures are maintained at a fixed level, whether the reactor is operating or not, by a judicious juggling of the power supplied to the heaters and the flow rate of coolant to the coolers.

To prevent local boiling of the coolant, the loop is pressurized by the surge tank which is merely a large vessel containing water and steam heated to a suitable temperature to provide the required pressure. The surge tank also acts as a reservoir to accommodate changes in the volume of the coolant caused by temperature changes. In addition, by initiating a flow of coolant through the vapor space of the surge tank and thence back to the loop, the surge tank may be operated as a very efficient degasifier.

On a bypass are found the ion-exchange resins which are used to maintain the purity of the water. Because these resins decompose at high temperatures the loop water must be cooled before it reaches them.

Table 2 shows typical conditions which can be maintained in a loop.

TABLE 2

LOOP OPERATING CONDITIONS

Pressure	Up to 2,000 psi
Coolant Temp.	Up to 570°F.
Linear Flow Past Fuel Specimens	Up to 20 (ft.) (sec.$^{-1}$)
Maximum thermal neutron flux	$\sim 4 \times 10^{13}$ (n) (cm^{-2}) (sec^{-1})

A variety of sizes and shapes of fuel may be irradiated in the test section. Rods up to 8 ft. long by $\frac{1}{2}$ in. in diameter may be irradiated or the same length of fuel can be subdivided into a "sausage chain" of short rods joined end to end. Flat plates have also been irradiated. Most work to date has been done on short rods of up to a foot long and roughly one half inch in diameter.

At present the UO_2 fuel is made by pressing UO_2 powder into cylindrical pellets at high pressures. These pellets are then sintered in a hydrogen atmosphere for several hours at a temperature of about 1700°C. The resultant ceramic has a density of about 10.5 gm./cc. (i.e. about 95% of theoretical). Fuel elements are made by slipping the pellets into Zircaloy tubes of the proper size and welding the ends closed.

Fuel examination facilities

Having irradiated the specimens under the correct conditions it is of course, imperative that they be examined to see how they have behaved. Thus the Remote Control Handling Facility, or "Cave" is a most important complement to the loop program.

It is possible to remove samples from the loops and take them in shielded containers, to the metallurgy cave which is shown in Figures 4 and 5. This is really a room surrounded with thick concrete walls into which are set thick lead glass windows. Remote handling manipulators pass through the walls and thus the specimens which are highly radioactive can be examined remotely. Table 3 shows some of the equipment which is used in the cave.

TABLE 3

APPARATUS IN CAVE

Stereo microscope and camera, (magnification 1x to 90x)
Micro-manipulator
Mechanical testers (Hardness, Bend Strength, Impact, Tensile)
Profilometer
Mechanical hack-saw
Lathe
Micro drill press
Grinding and polishing wheels (for metallographic work)

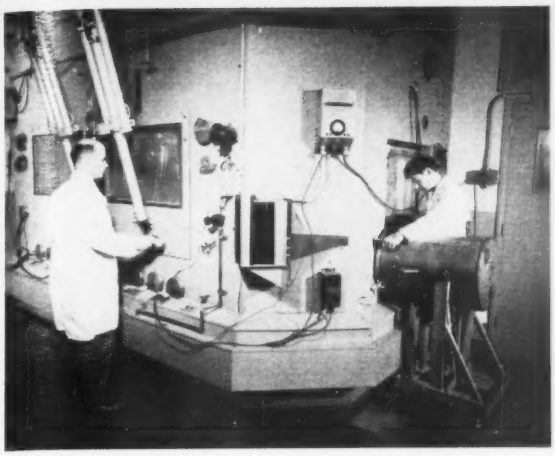

Figure 4—Photograph of remote handling cell.

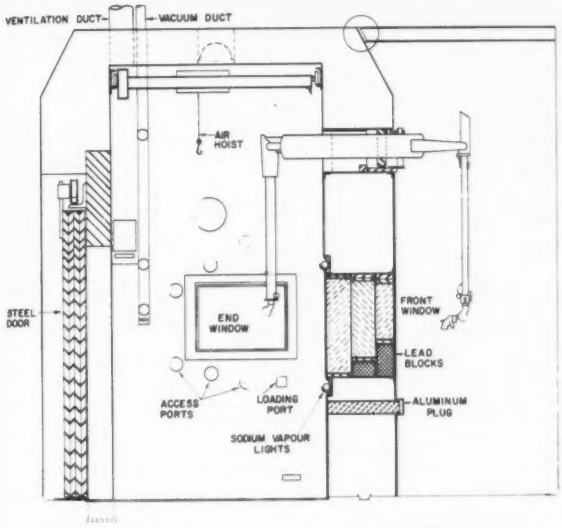

Figure 5—Vertical section of remote handling cell.

Experimental investigations

The discussion of experiments carried out at Chalk River using these facilities will be limited to the testing of UO_2 and sheathing materials suitable for use in future water cooled power reactors.

1. *Irradiation behavior of UO_2*

Of course one of the most important questions is:—"How does the oxide stand up to irradiation?" In this connection it must be remembered that because a large amount of energy is being released in the fuel by the fission process and because dense UO_2 is a relatively poor conductor of heat, very large temperature gradients will occur throughout the fuel. The centre may well be at a temperature rather close to the melting point of 2800°C., whereas the surface of the element will be less than 500°C. This is a temperature gradient of about 9000°C. per inch. Many specimens of UO_2 have been irradiated in order to determine the effect of high thermal neutron flux and the consequent high temperature gradient, on the fuel.

In most instances UO_2 has withstood the irradiation very well, and beyond some cracking, caused probably by thermal shock, the pellets appear visually and dimensionally unchanged even after quite long irradiations. Figure 6 shows a typical example.

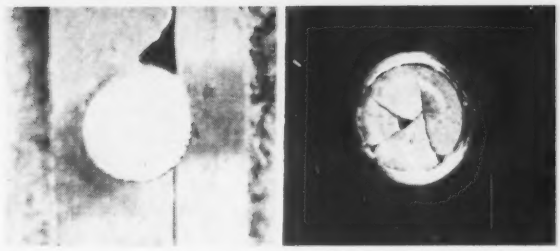

Figure 6—Two samples of compacted and sintered UO_2. Both irradiated to about 4800 MWD/Tonne UO_2. One has cracked and the other is uncracked. (1 Tonne = 10^3 kilograms)

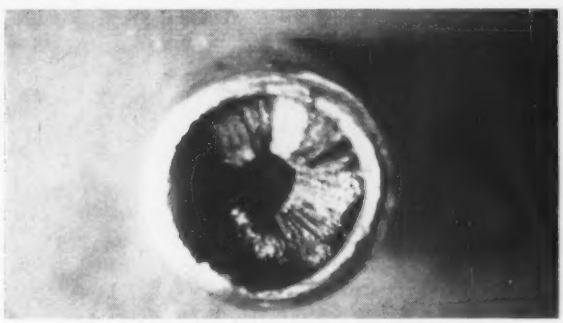

Figure 7—Compacted and sintered UO_{2+x} irradiated to about 4800 MWD/Tonne UO_2 shows formation of central flue.

In some samples, in which the core temperature has been over an estimated 1600°C., grain growth at the centre of the pellet has been seen. In other samples, of composition UO_{2+x} the interesting phenomena shown in Figure 7 has been seen where a large central "flue" has been formed down the centre of the specimen, and long crystals radiate from this flue to the edge of the specimen. There is still much speculation as to the exact nature of the process occurring in these specimens, some believe it to be melting while others believe it to be a mass transport phenomenon.

However, it is now possible to tell the reactor designers that as long as certain conditions are met (and some of these conditions can be outlined quite specifically), UO_2 is a fuel which will withstand long irradiations without swelling or distorting in any way.

2. *Fission product gases*

Among the products of fission are stable isotopes of the rare gases Kr and Xe. At the high temperatures found in the fuel, atoms of these gases can diffuse from the oxide lattice and collect in the space between the fuel and the sheath. After a very long irradiation it is possible that enough of these gases may have collected in this space to give high pressures inside the sheath and consequent deformation or rupture. To study this question, specimens of fuel in Zircaloy sheaths are irradiated and after irradiation the sheath is punctured in a specially constructed apparatus in the cave and the amount of gas released is measured.

To date this problem of pressure build-up does not appear to be a serious one from a practical standpoint, but much information is being obtained regarding the actual mechanisms of release and subsequent history of these gases.

3. *Defect tests*

Information is being obtained on the release of fission product gases and also of other fission products by irradiating samples in which the Zircaloy sheath has been punctured by drilling a small hole through it to the fuel below. By analysing the loop water, it can be determined which isotopes escape most readily, the extent to which they escape and also their subsequent history in the loop. In other words, do they remain in solution, do they end up on the ion exchange resins or do they deposit on the walls of the loop piping?

Studies such as these give information on several other problems such as:—

(i) Is the oxide stable to high temperature water and to steam?

(ii) What will the problems be in an operating reactor if the fuel sheath ruptures and what necessary steps must be taken for decontamination?

(iii) What is the most suitable monitoring system to give early warning of sheath failure?

4. *Corrosion studies*

To date an alloy of zirconium and tin, known as Zircaloy-2 appears to be the most promising sheath for enclosing UO_2 fuel because it combines desirable nuclear properties with good resistance to corrosion by high temperature water. Figure 8 shows the exterior of a Zircaloy sheated specimen after an exposure in loop water at a temperature of 500°F. for several months. The original machining marks are clearly visible, and obviously no corrosion has taken place and no fouling of the surfaces has occurred.

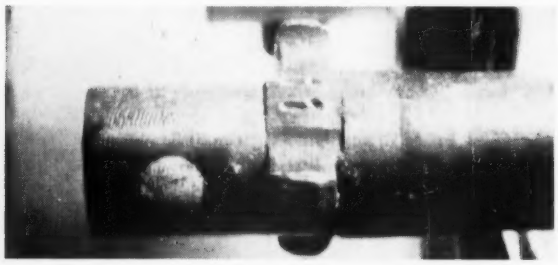

Figure 8—End of Zircaloy-2 sheathed fuel specimen — exposed to water at 525°F. for four months.

There are problems associated with Zircaloy, however. One problem is that, as well as using Zircaloy as a sheath material for the fuel, it is proposed to use it in the pressure tubes of NPD-2, which must have a lifetime of at least t n years. When Zircaloy is in contact with water at 500°F. a dark highly protective film of ZrO_2 forms over the surface resulting in a low corrosion rate ($\approx 1.4 \times 10^{-5}$ in/yr) which is independent of such factors as water velocity etc. However after a certain time which is not definitely known but will probably be about eight years under NPD water conditions, the protective oxide layer changes to a white less protective oxide. The corrosion rate is still low ($\approx 2.5 \times 10^{-5}$ in./yr.) but whether it is now dependent on such factors as water velocity is not known for certain. Tests are now being conducted in which the transition of black to white oxide has been induced to occur in a short time by treatment of the metal in steam at 750°F. These specimens, with the transition film, are now being tested with water at 500°F. moving past them at 20 ft./sec. to see whether the resultant corrosion rates are acceptable.

Although Zircaloy-2 is a good sheathing material, it is expensive. The search for a cheaper sheathing material is continuing and a number of alloys of aluminum with nickel are being studied. These alloys have quite low corrosion rates (≈ 0.003 in./yr.) in water at 500°F. provided certain conditions are fulfilled. This rate is just acceptable for a fuel sheath provided that the alloy is not susceptible to pitting and providing it is not necessary to irradiate the fuel for too long a time. The processes occurring are not yet fully understood but it is hoped that by the addition of corrosion inhibitors to the water corrosion rates can be decreased.

In this paper only the highlights of the AECL testing program have been considered. Appended is a list of pertinent AECL reports, all of which are unclassified, which give fuller details of various aspects of the program.

Reference

(1) Allison, G. M., C.J.Ch.E. 36: 217-220: Oct. '58. (AECL Report DCI-30).

AECL Reports on Loop Tests, etc.

Booth, A. H., "A Method of Calculating Fission Gas Diffusion from UO_2 Fuel and its application to the X-2-f Loop Test." AECL Report CRDC-721 (AECL No. 496), Sept. 1957.

Booth, A. H., Bain, A., Rymer, G. T., Kerr, D. B., "Collection and Measurement of Stable Fission Xenon in Sheath Puncture Experiments —Method and Results to Date." AECL Report CRDC-719, Oct. 1957.

Booth, A. H., "A Suggested Method for Calculating the Diffusion of Radioactive Rare Gas Fission Products from UO_2 Fuel Elements." AECL Report DCI-27, Sept. 1957.

Tomlinson, M., Robertson, R. F. S., Pattison, J., "The Chemistry of the first AECL Fuel Rod Test in the WAPD-CR-IV-X2 Loop." AECL Report CRDC-650, June 1957.

Robertson, R. F. S., Krenz, F. H., "Defect Test on U-2 w/o Zr Alloy in the X-2 Loop. Test No. 1." AECL Report CRDC -646 (AECL No. 366), April 1956.

Robertson, R. F. S., "Defect Test on U-2 w/o Zr Alloy in the X-2 Loop. Test No. 2." AECL Report CRDC-647.

Robertson, R. F. S., G. M. Allison, "Irradiation of Compacted and Sintered UO_2 in the X-2 Loop Tests X-2-f and X-2-i." AECL Report CRDC-718, May 1958.

Robertson, R. F. S., "Review of Loop Programme in the NRX Reactor." AECL Report UK/C-6-101, Sept. 1957.

Howieson, J., "A Report on the First NPD Single Element Irradiation and Failure." AECL Report CRNE-744 (AECL No. 552), August 1957.

Bain, A. S., Payne, W. E., Howieson, J., "Irradiation of UO_2 and U-2 w/o Zr Alloy in the CR-V Loop." AECL Report NEI 84, Feb. 1958.

Bain, A. S., "Construction and Shielding Properties of Remote Control Handling Cell, Metallurgy Building, Chalk River, Ontario." AECL Report CRL-39, March 1957.

Krenz, F. H., "The Corrosion of Aluminum-Nickel Type Alloys in High Temperature Aqueous Service." AECL Report CRL-40, May 1957.

Krenz, F. H. et al, "Chalk River Experience with Zircaloy-2 and Aluminum-Nickel-Iron Alloys in High Temperature Water." Paper No. P/194 submitted to the Second United Nations International Conference on the Peaceful Uses of Atomic Energy, Geneva, Sept. 1958.

Chalder, G. H. et al, "Fabrication and Properties of Uranium Dioxide Fuel." Paper No. P/192 submitted to the Second United Nations International Conference on the Peaceful Uses of Atomic Energy, Geneva, Sept. 1958.

Robertson, J. A. L. et al, "Behaviour of Uranium Oxide as a Reactor Fuel." Paper No. P/193 submitted to the Second United Nations International Conference on the Peaceful Uses of Atomic Energy, Geneva, Sept. 1958.

* * *

Conditioning of D_2O in Heavy Water Power Reactors[1]

G. M. ALLISON[2]

This report indicates the problems associated with the maintenance of the purity of the D_2O in a pressurized heavy water power reactor and how these problems are handled.

In a pressurized water power reactor, impurities will be introduced into the coolant and moderator from the corrosion of the steel system. These impurities are mainly particulate and colloidal in nature. They must be kept to a minimum since when circulated through the reactor they become activated by the neutron flux and when deposited throughout the system they make accessibility for maintenance difficult. Impurities may also be introduced into the water from fuel element ruptures. These also create maintenance problems since they are intensely radioactive.

Heavy water systems require a constant guard against the introduction of light water which would degrade the D_2O and make the operation of the reactor inefficient or perhaps impossible. The isotopic content of the heavy water must be checked constantly. Upgrading may be required periodically or continuously.

The general purity of the water in the reactor is maintained by passing a fraction of the main circulating volume through a by-pass containing a filter and a mixed bed ion exchange resin column. This column serves to remove ionic impurities as well as acting as an efficient filter itself. It is also used to maintain the pH of the water at the desired level whether neutral or alkaline. In the case of heavy water systems the resin must be deuterized before use to prevent degrading the D_2O.

A PRESSURIZED heavy water power reactor essentially consists of a closed system in which heavy water coolant is heated by the fuel rods and is circulated through heat exchangers and back to the reactor vessel again. Boiling is prevented by pressurizing the system. A simple diagram of such a system is shown in Figure 1 of reference 1. The out-reactor parts of this system are mild steel and the in-reactor pressure tubes are made of Zircaloy-2 (a zirconium-tin alloy).

There are several ways in which impurities can be introduced into the D_2O.

(1) The main impurities in the system will be the corrosion products (so-called "crud") which are formed in the reaction between the hot water and the metal surfaces. This crud will be present mainly in colloidal and particulate forms and to a very slight extent as ionic material. These are the same corrosion products that one finds in a conventional steam plant.

(a) (b)

Fuel elements showing deposited crud after irradiation for one month in pH7 water at 525°F., conductivity < 1 umho cm^{-1}.

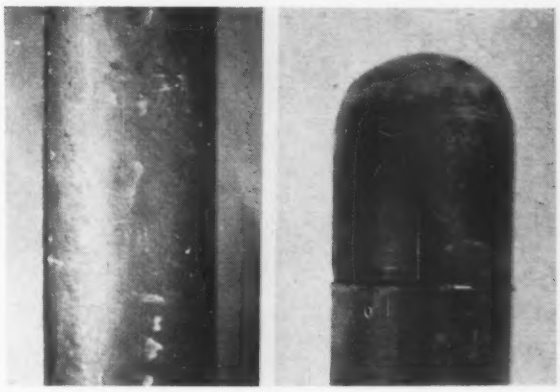

(c) (d)

(c) Fuel element after irradiation for one month in pH7 water, 2×10^{-4} M in K_2SO_4, at 525°F.

(d) Fuel element after irradiation for two months in pH10 water at 525°F.

Figure 1

(2) Fission products will be present from the fissioning of uranium occurring as an impurity in the Zircaloy-2 and as so-called "tramp" uranium on the surface of the sheathed fuel. This tramp uranium is very difficult to remove completely after fabrication of the fuel elements. Fission products will also be introduced into the coolant when fuel element failures occur.

(3) Light water if introduced into the system will degrade the D_2O.

[1]*Manuscript received July 25, 1958.*
[2]*Associate Research Officer, Chemistry and Metallurgy Division, Atomic Energy of Canada Limited, Chalk River, Ont.*
This article is based on a paper presented at the Joint A.I.Ch.E.-C.I.C. Chemical Engineering Conference, Montreal, April 20-23, 1958.

The crud problem

In any power reactor employing light or heavy water at high temperatures corrosion products will cause certain problems which are the same as those in a conventional steam plant and others which are characteristic only of nuclear plants. In steel systems, crud is formed by corrosion reactions and is composed mainly of magnetite, Fe_3O_4, with small amounts of the oxides of the alloying metals in the steel, Cr, Ni, Mn, etc. The number and amount of the alloying elements appearing in the crud will depend on the composition of the steel, mild steel crud being nearly pure Fe_3O_4. If oxygen is present in the water Fe_2O_3 will also be present.

Some of the corrosion products will remain on the metal surface as a corrosion film while some will be released to the water and carried throughout the system mainly in particulate and colloidal form. In a conventional steam plant this material can be detrimental in many ways.

(a) The particulate crud can build up in places causing reduction in flow rate.

(b) It can cause wear and malfunction of moving parts made to close tolerances.

(c) It can deposit on heat transfer surfaces.

Nuclear plants also have these problems and in addition they have two more–

(d) Under certain water conditions, crud will preferentially deposit on the fuel elements causing reduction in heat transfer rates and possible over-heating of the fuel with subsequent burnout.

(e) Corrosion products become activated by absorption of neutrons in the reactor and are deposited throughout the out-reactor parts of the system. These activation products are γ-emitters and many have sufficiently long half-lives to cause maintenance problems.

Pressurized water nuclear power plants then will have more problems due to corrosion products than conventional steam plants. It must be remembered that in nuclear plants amounts of crud which would be considered insignificant in a conventional steam plant can cause serious problems due to radioactivity and to preferential deposition on the fuel elements.

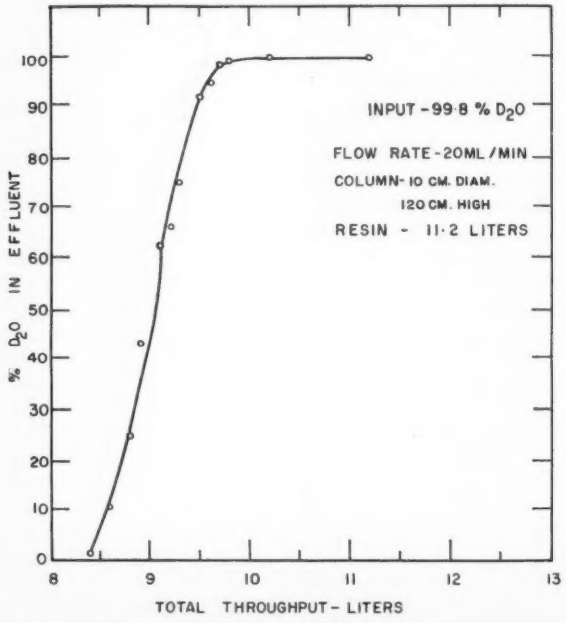

Figure 2—Resin deuterization curve.

It is thus desirable to keep the crud concentration in the water as low as possible and to choose water conditions which will also prevent preferential deposition on the fuel. Considerable data on the behavior of crud in stainless and mild steel systems containing high temperature water at high pressure have been obtained from the loops described by Robertson [1] where simple flow diagrams of a typical loop are shown in Figures 2 and 3. It has been shown quite definitely in loop experiments in the NRX reactor at Chalk River and in American reactors, that maintaining the high temperature water at pH 9.5 - 10.5 with KOH or LiOH keeps the crud level in the water low, prevents the preferential deposition of the corrosion products on the fuel elements and removes any crud which may have been deposited under former, less desirable, water conditions [2, 3]. It has also been shown that neutral water which has been made 2×10^{-4} M in potassium sulphate has the same effect as high pH water [2]. The effect of potassium sulphate has been shown in one loop test only while that of KOH has been substantiated many times. More K_2SO_4 experiments are required. Table 1 contains results obtained in loop experiments in NRX in which different water conditions prevailed. The effect of high pH and K_2SO_4 on the crud level in the water can be readily seen.

TABLE 1

EFFECT OF WATER CONDITIONS ON CRUD LEVELS IN LOOPS

Water Condition	Crud Level, ppb*
pH 7, conductivity < 1 μmho (Stainless Steel)	10–50
pH 7, 10^{-4} M K_2SO_4 (Stainless Steel)	1–5
pH 10, KOH (Stainless Steel)	2–10
pH 10, KOH (Mild Steel)	10–50

*ppb = parts per billion.

Large variations in the crud level are often caused by thermal cycling of the loops from reactor trips and start-ups and from deliberate cooling of the loops for maintenance purposes. Temperature changes tend to crack the corrosion film causing crud to be released to the loop water. In one of the mild steel loops the crud concentration under high pH water conditions has risen to over 1000 ppb for short periods due to thermal cycling.

Photographs of Zircaloy-2 clad UO_2 fuel elements which were irradiated under conditions given in Table 1 are shown in Figure 1 [2]. The effect of water conditions on the deposition of crud on the fuel can be readily seen.

Radiation problems

(a) **Active crud:** Besides the physical problems pertaining to crud which have just been considered, there is also an activity problem. Corrosion products when exposed to a neutron flux in the reactor vessel become radioactive. The extent of the activity will depend on the absorption cross section of the material for neutrons, the length of time in the neutron field and the half-life of the radionuclide formed.

Active corrosion products found on pipe walls outside the reactor vessel can come from three sources:

(i) from corrosion of active metal in the reactor vessel, the active crud being carried throughout the system in the circulating water,

(ii) from activation of crud formed outside the reactor but deposited within the reactor vessel for a time and then transferred throughout the system,

(iii) from crud being activated as it is repeatedly carried in and out of the reactor in the recirculating water.

The last source is insignificant compared to the other two.

Table 2 shows the major corrosion product activities found in crud samples collected from the recirculating water in a stainless steel loop in NRX.

TABLE 2

γ-EMITTING ACTIVATED CORROSION PRODUCTS

Nuclide	Half-Life	Mode of Formation	% of total γ-activity in crud sample after 7 days
Fe^{59}	45 d	neutron capture by Fe^{58}	5–15
Mn^{56}	2.6 hr	neutron capture by Mn^{55}	Only a major contributor for the first 24 hours
Co^{58}	71 d	neutron capture by Ni^{58*}	10–20
Co^{60}	5.2 yr	neutron capture by Co^{59}	
Cr^{51}	27 d	neutron capture by Cr^{50}	10–20
Sb^{122}	2.8 d	neutron capture by Sb^{121}	10–20
Sb^{124}	60 d	neutron capture by Sb^{123}	
Zr^{95}	65 d	neutron capture by Zr^{94}	40–50 (Zr^{95} + Nb^{95})

*In this case neutron capture is followed by a proton emission instead of a γ-ray.

Although antimony is a very minor constituent in steels it has a large absorption cross-section for thermal neutrons and antimony activities have been found to be major contributors to the long-lived γ-activity in crud collected from the water in both stainless and mild steel loops in NRX. They can also be formed by a (p,n) reaction on the tin in the Zircaloy. Zr^{95} comes from the activation of zirconium in the Zircaloy-2 used to clad the fuel elements and used as structural material for the pressure tube in this particular loop. Nb^{95} is the daughter of Zr^{95} and is also a γ-emitter (half-life 35 d).

It can readily be seen that a build-up of long-lived γ-emitting active corrosion products on pipe walls could cause maintenance problems due to parts of the system becoming inaccessible except for short periods. The maximum permissible total body irradiation which anyone is allowed is 5 roentgens (r)* per year which is roughly an average of 100 milliroentgens (mr) per week. A man working in a general radiation field of 1 r/hour therefore, will receive his week's dosage in 6 minutes. As we will see later, high fields are experienced in loops when fuel element ruptures occur. From the activity stand-point, it is thus important to keep the crud release rate and the corrosion rate low by using proper water conditions to minimize the transfer of crud throughout the system.

(b) **Activation products of water:** The water in a pressurized water reactor will become very radioactive due to neutron activation of O^{16} to form N^{16} (half-life 7.3 seconds), and O^{17} to form N^{17} (half-life 4.1 seconds). If the water is not deaerated, natural A^{40} will be present and be activated to form A^{41} (half-life 1.8 hours). Some F^{18} (half-life 1.9 hours) is also formed from O^{18} by a (proton, neutron) reaction. Fortunately, these activation products are short-lived and do not cause radiation problems shortly after the reactor shuts down. They do, however, necessitate shielding of piping containing cooling water circulating between the reactor and heat exchangers.

*The roentgen is a frequently used unit of radiation dose.

(c) **Fission product activities:** Fission products will be present in the cooling water in a power reactor due to uranium impurities in the fuel sheathing material and pressure tubes and due to "tramp" uranium on the sheaths. However, the major source of fission products will be from ruptured fuel elements, i.e. where the sheaths fail.

Loops in NRX have been operated with deliberately defected fuel elements in order to study the release of fission product activity from different types of fuel and to study the behavior of the different fission products in the cooling water. By passing a portion of the main loop flow through a mixed bed ion exchange column, a much lower equilibrium activity level in the loop water can be attained for the longer-lived fission products ($t_{½}$ > a few hours) than if no ion exchange is used at all. If the fission product source is removed, the water can be cleaned up satisfactorily by the resin column.

Some fission product activities tend to deposit on pipe walls with the corrosion products. These are mainly the more insoluble elements. Table 3 shows the major γ-emitting active nuclides found deposited on pipe walls in a loop in NRX when defected UO_2 elements were present. In this loop the in-reactor pressure tube was stainless steel.

TABLE 3

MAJOR γ-EMITTING NUCLIDES DEPOSITED ON PIPE WALLS IN DEFECT TEST

Niclide	Source		Half-Life	Relative % of Total γ after 4 days
	Fiss. Prod.	Crud		
Mo^{99}	x		67 hr	55
Sb^{124}		x	60 d	10
Co^{60}		x	5.2 yr	9–10
Fe^{59}		x	45 d	4
Ru^{103}	x		40 d	2
Te^{129}	x		33 hr	1–2
Te^{132}	x		77 hr	
Ba^{140}	x		12.8 d	0.5–1
Cr^{51}		x	27 d	0.5–1
Zr^{95}	x	x	65 d	0.5–1

The piece of pipe removed from the loop for analysis was Type 304 Stainless Steel, 1 in. Schedule 80, and had had loop water flowing through it at 10 U.S. gpm for 2 months. The radiation field on contact with this pipe when removed from the loop was ≈ 20 mr/hr.

The defect test in this loop lasted for approximately 14 months. At the end of the test a piece of pipe which had been onstream the whole time was removed from the loop and the corrosion product film removed by brushing and acid etching. It was found that the relative amounts of fission product and corrosion product activities were entirely different to those listed in Table 3, viz. Co^{60} accounted for ≈ 50%, and Mo^{99} ≈ 30% of the total γ-activity after four days.

Decontamination after fuel element ruptures

Fuel element ruptures occur occasionally in loop tests causing very high activity levels in the loop water. When this happens with UO_2 fuel elements, the activities released to the coolant are mainly rare gases and water

soluble fission products such as the kryptons, xenons, cesiums, iodines, etc., unless the rupture is severe enough to allow particulate UO_2 to be spread throughout the loop. Draining the loop followed by refilling and circulating through fresh ion exchange resins greatly reduces the radiation level. For example, when a UO_2 fuel element ruptured in a loop at NRX at the end of February, 1957 [1], the activity in the loop water rose by a factor of 500 and radiation fields in contact with loop piping were in the order of 75 roentgens (r)/hr. (normal field < 0.1 r/hr.). Using the above treatment for decontamination the radiation field on the loop piping was brought back to normal in about a week. Simply draining the loop shortly after the rupture occurred reduced the field to about 1 r/hr.

In another similar case of a UO_2 fuel element rupture, two other decontaminants were tried as well as water—namely, periodic acid and citric acid. Results indicated that neither of the acids was any better as a decontaminating agent than water alone. Versene has been tried at different pH's as a decontaminating agent with similar results.

In reactors, especially those employing heavy water, such draining and flushing techniques are not practical. Decontamination must be carried out by degassing and ion exchange methods. If UO_2 fuel is used and the oxide is retained in the fuel element there should be no decontamination problem. However, if UO_2 should be released to the water it will tend to deposit throughout the system and will create an additional clean-up problem. This is at present commanding considerable attention.

In NRX itself fission product contamination of the heavy water occurred in July, 1955, from the rupture of a plutonium fuel rod. In this case the major decontamination of the D_2O was accomplished by means of ion exchange resins.

The use of ion exchange resins in the maintenance of D_2O purity

It has been found in the operation of the NRX reactor and of high temperature loops in the reactor that high water purity can be maintained most readily by passing a fraction (about 1%) of the main recirculating volume through a by-pass containing a filter and an ion exchange resin column. Usually a mixed bed resin is used consisting of a strongly acid cation exchange resin and a strongly basic anion exchange resin. Besides removing ionic impurities, the resin column is itself an efficient filter. When the mixed bed resin is in the H-OH form, the water is kept at pH 6.5-7.0 and conductivity < 1 umho cm^{-1}.

In heavy water systems, the resin must be deuterized before being used—i.e. the water and exchangeable H and OH groups must be replaced by D_2O, D and OD, to avoid degrading the D_2O. This is usually done by packing a glass column with the resin in light water. Heavy water (ca. 99.5% D_2O) is introduced at the bottom of the column and allowed to displace the H_2O from the column. With a flow rate of 20ml/min. for a 10 cm. diameter column there is very little mixing at the interface of the D_2O and H_2O. When all the light water has been displaced from the column, high grade heavy water is flowed through (ca.99.8%D_2O). When no further degradation of the D_2O coming from the top of the column is observed, the flow is stopped and the resin removed and stored in a sealed container. The amount of 99.8% heavy water degraded is usually about 2 kg. per 7 kg. of resin deuterized. A typical resin deuterization curve is shown in Figure 2.

The resin also serves to maintain the pH of the water in the system at the desired level. If neutral water is desired, the resin is used in the H-OH form. If alkaline water is desired, at pH 9.5-10.5, the resin is used in the K-OH or Li-OH form. In the loop experiments at Chalk River, high pH is used almost entirely to avoid the buildup of crud on the fuel elements.

The size of the resin column that is used in any particular system will depend on the purity required, the rate of production of impurities, the clean-up time required, etc. Standard ion exchange practices are followed—i.e. for optimum performance the flow rate should be 2-10 U.S. gpm per ft^3 of resin (minimum bed depth 24 in.).

Ion exchange resins, therefore, can serve several purposes in a pressurized heavy water power reactor:

(1) They maintain the pH at the desired level.

(2) They help keep fission product activity at a low equilibrium level.

(3) They help keep the crud concentration in the water low, by adsorption of charged corrosion products, ionic or colloidal, and filtration of particulate crud.

(4) They serve as decontamination agents when fuel ruptures occur.

Upgrading of heavy water

In any heavy water reactor the isotopic purity of the D_2O must be kept above a certain level or the reactor will not operate without the addition of enriched fuel. It is therefore necessary to have some means of upgrading the D_2O, either intermittently or continuously.

In the NRU reactor at Chalk River it is planned to upgrade continuously, if this is necessary, using either a bubble cap plate column or a sieved plate column. The column will be fed from a sidestream with 99.76% D_2O which will be returned to the reactor as 99.80% D_2O.

The heavy water in the NRX reactor does not require continuous upgrading. If accidental downgrading takes place the D_2O is reconcentrated by electrolysis. A current of 1000 amperes at 3 volts is used in each of 4 cells. The average grade of D_2O reconcentrated is 97% providing a product (60% of the feed) which is about 99.9% D_2O. The gases leaving the top of the cells are recombined for future feed. The minimum grade of heavy water handled is 80% D_2O. To provide passage for the large current the feed is made 1.5% KOH and 1.0% K_2CO_3.

Conclusion

Results from experimental work in loops have indicated that a pressurized water power reactor should be operated if possible with the coolant at high pH to minimize the problems created by corrosion products. Continuous side-stream purification with mixed bed ion exchange resin columns is desirable to keep the crud concentration in the water low, to minimize the equilibrium fission product activity level, to maintain the desired pH and to clean up water soluble activity resulting from fuel ruptures.

Some means of upgrading D_2O is desirable for heavy water reactors for intermittent or continuous use.

It should be emphasized that the results reported here have been obtained on small light water loop systems and these results may not be the same as will be obtained in a power reactor.

References

(1) Robertson, R. F. S., C.J.Ch.E. 36: 213-216: Oct. '58.
(2) Robertson, R. F. S., and Allison, G. M., AECL Report No. CRDC-718.
(3) Glick, H. L., Westinghouse Atomic Power Division, Report No. WAPD-113.
(4) Howieson, J., AECL Report No. CRNE-744.

★ ★ ★

End Effect Corrections in Heat and Mass Transfer Studies[1]

A. I. JOHNSON[2], *A. HAMIELEC*[3], *D. WARD*[3] *and A. GOLDING*[3]

Recently, considerable effort has been made to investigate mechanisms of heat and mass transfer to drops or bubbles passing through a continuous liquid medium. Many of these studies have been hampered by the unavailability of accurate methods for determining end effects.

This paper outlines methods of plotting efficiency measurements for the overall transfer process so that both the magnitude of the end effects and the mechanism of the steady fall or rise period may be investigated. The examples are drawn from mass transfer with resistance inside the dispersed phase and from heat transfer with resistance in both phases. For resistance in one phase the methods are straight line extrapolations.

Various mechanisms of transfer inside drops have been studied to test the methods of determining end effects.

During recent years several studies have been made on the heat and mass transfer rates to and from drops or bubbles passing through continuous fluids. These studies have been directed at examining mechanisms for the transfer processes inside the drops or bubbles, or from these, during the steady fall or rise of the dispersed phase. Here "steady" infers that the transfer mechanism inside and outside the drop or bubble is constant with respect to the drop or bubble.

These studies have usually been carried out by forming the dispersed phase, allowing it to rise or fall and then to coalesce (or burst in the case of bubbles) all in contact with the continuous phase. Different transfer processes are occurring during all three states of the drop or bubble. In order to measure the transfer during the steady rise or fall period, end effect corrections for the other periods must be made.

There have been several methods of evaluating these end effects. This paper will review these and propose modified techniques for combining end effect analysis and examination of the transfer mechanism. As far as possible, an attempt has been made to obtain straight line extrapolation techniques.

Previous work

Among the first investigators reporting end effects in liquid-liquid extraction were Johnson and Bliss [1], Sherwood, Evans and Longcor [2], Treybal [3], and West, Robinson, Morgenthaler, Beck, and McGregor [4].

Sherwood, Evans, and Longcor determined a drop formation end effect by plotting the logarithm of the fraction unextracted based on the concentration of the solvent phase, against column height. The resulting straight line was extrapolated to zero column height to give an end effect of approximately 40% of the total material transferred. Using this procedure, West, Robinson, Morgenthaler, Beck, and McGregor repeated the work of Sherwood, Evans, and Longcor and found with a similar plot a formation end effect of about 20%. The reason for this inconsistency was probably due to direction of transfer.

Licht and Conway [5] have indicated that a study of the mechanism of solute transfer should recognize three separate stages of extraction in the life of each drop during spray tower operation. The period during which the drop is forming on the tip constitutes stage 1. Stage 2 covers the period of drop fall (or rise) through the continuous phase. Stage 3 includes the coalescence of the drop and any interface transfer at the opposite end of the tower. They have attempted to determine formation and coalescence end effects separately, using a specific apparatus for eliminating the coalescence end effect. Licht and Conway plotted percent extracted for the disperse phase versus column height to determine end effects. However, for several cases encountered the plots were curved, but were extrapolated as straight lines. The end effects thus determined were probably not very accurate.

Licht and Pansing [6] concluded that the amount of extraction occurring during drop formation is sufficiently small so that experimental results do not detect the variation with drop formation time. They also state that unless the final end effect is eliminated any extrapolation procedure is incorrect.

Coulson and Skinner [7] developed an ingenious apparatus for determining the amount of transfer occurring during drop formation. Drops were formed on the end of a capillary and then withdrawn before breaking away. Their technique did not measure the transfer caused by drop deformation as a drop is detached from the orifice.

Pang Sheng Li [8] reported end effects for absorption from bubbles of various gases.

Geankopolis and Hixon [9] measured the mass transfer rates in various sections of a liquid-liquid extraction column by sampling the continuous phase by means of a moving probe. They reported a large end effect at the continuous phase entry-end. A similar study on a second system was reported by Geankopolis, Wells and Hawk [10]. Gier and Hougen [11] made a similar study of spray columns in liquid-liquid extraction and reported large circulation effects caused by rising liquid drops.

[1]*Manuscript received March 27, 1958.*
[2]*Associate Professor of Chemical Engineering, University of Toronto, Toronto, Ont.*
[3]*Graduate students, Department of Chemical Engineering, University of Toronto, Toronto, Ont.*
Contribution from the Department of Chemical Engineering, University of Toronto, Toronto, Ont.

Apparatus

The apparatus used in this study is shown in Figures 1 and 2.

Figure 1 illustrates the apparatus in which the transfer of n-butyl alcohol into falling drops of water has been studied. The same apparatus without the linseed oil separating phase was used to obtain data for the transfer of cyclohexanol from a continuous phase of cyclohexanol saturated with water to falling water drops. It consisted of a glass cylinder 3 in. inside diameter and 3 ft. long tapered at the bottom to a stopcock through which coalesced disperse phase could be withdrawn.

It was found that drops of water greater than 0.00900 ft. in diameter would not form well in the continuous phase of n-butyl alcohol saturated with water and had to be formed in air above the continuous phase. However, for the water-cyclohexanol system all water drops were formed in the continuous phase. The single dispersed phase drops were formed from sharp-edged stainless steel nozzles 5/16", 1/4", 3/16" and 1/8" inside diameter, as well as from a number of hypodermic needles [17]. Drop diameters were determined by counting the number of drops required to make a volume of approximately 7 cc., assuming the drops to be spherical.

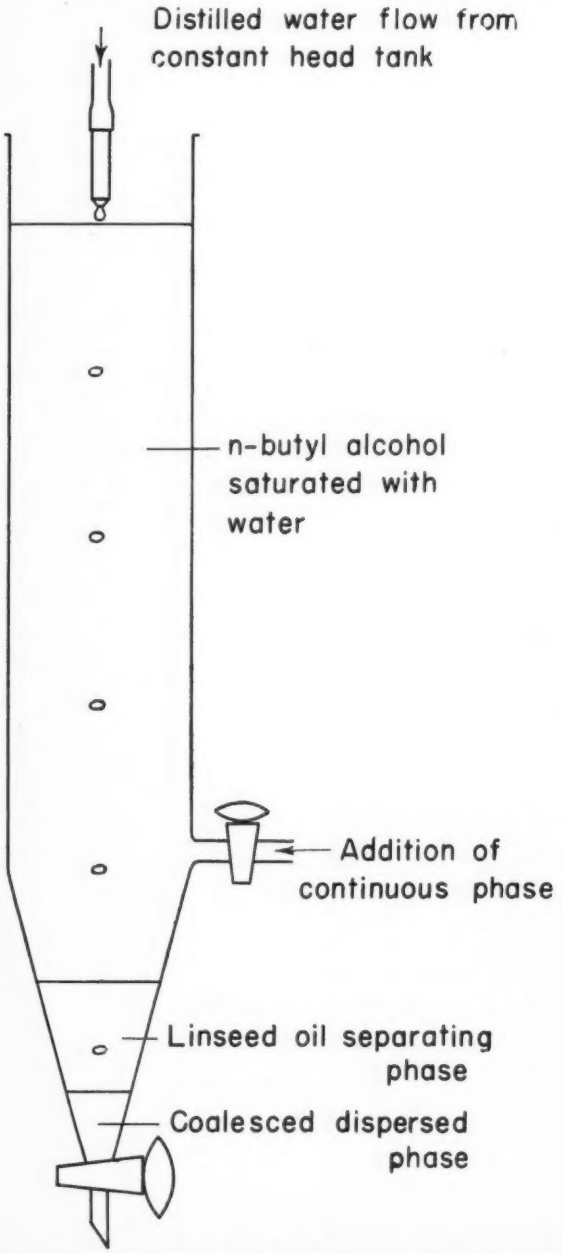

Figure 1—Apparatus for measuring mass transfer rates inside drops, showing second immiscible phase for eliminating the settling end effect.

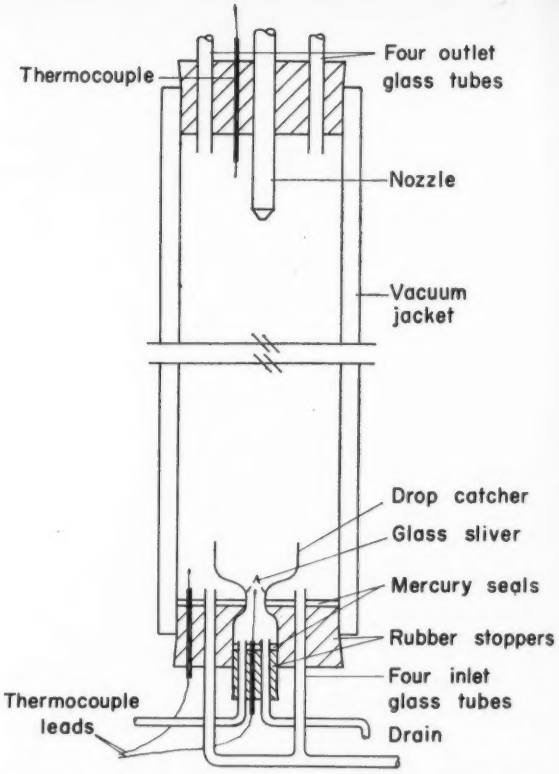

Figure 2—Apparatus for measuring heat transfer rates from or to drops, with resistance in both phases.

In an attempt to eliminate the coalescence end effect, linseed oil was carefully run in under the continuous phase (n-butyl alcohol saturated with water), to act as a separating layer.

The amount of solute transferred to the drops was measured by the refractive index change of the collected disperse phase.

Figure 2 illustrates the apparatus in which the heating and cooling of dispersed phase falling through a continuous phase was observed. The apparatus was essentially the same as that used by Korchinski [12] except that the nozzle was jacketed throughout its length. It was found advantageous to have the drops fall on a glass point in the drop catcher, to decrease the time required for drops to coalesce and thus decrease the end effect. This column had an inside diameter of 37 mm. and was 53 cm. long. The length of the column for drop fall was varied by adjusting the position of the nozzle in the column. Copper-constantan thermocouples were used to measure temperature.

Calculation techniques

The calculation techniques discussed in this section will be illustrated later by both mass and heat transfer

experiments. For brevity, the definitions and equations given in this section refer to mass transfer operations only.

a) **End effect definitions:** The following definitions may be stated:

$$E_{f1} = \frac{C_1 - C_2}{C_1 - C^*} \quad \ldots\ldots(1)$$

$$E_{f2} = \frac{C_3 - C_4}{C_3 - C^*} \quad \ldots\ldots(2)$$

$$E_m = \frac{C_2 - C_3}{C_2 - C^*} \quad \ldots\ldots(3)$$

$$E_T = \frac{C_1 - C_4}{C_1 - C^*} \quad \ldots\ldots(4)$$

where the various concentrations have been defined on Figure 3, with the exception of C^* which is the equilibrium concentration of disperse phase reached after an infinitely long contact with the continuous phase. For any run C^* is a constant.

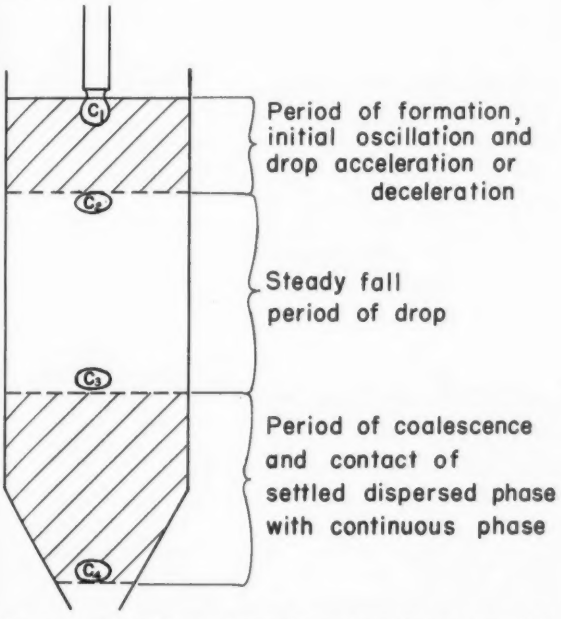

Figure 3—Definitions of transfer regions during drop fall.

Here E_m is the fractional approach to equilibrium during the steady rise or fall period. It is for this period that one wishes to be able to test various mechanisms.

On the other hand E_T is the fractional approach to equilibrium calculated by taking measurements on the entering and leaving dispersed phase.

The initial end effect E_{f1} may include several transfer mechanisms—transfer inside or at the nozzle and excessive transfer rates during the unsteady period usually occurring after drop release. The effect E_{f2} is that observed during coalescence and may include transfer to the settled dispersed phase. Normally for experiments at constant drop size and formation rate E_{f1} and E_{f2} are independent of column height.

From the definitions above, the following may be obtained algebraically:

$$E_m = \frac{E_T - E_{f1} - E_{f2} + E_{f1} \times E_{f2}}{1 - E_{f1} - E_{f2} + E_{f1} \times E_{f2}} = \frac{E_T - E_F}{1 - E_F} \quad \ldots\ldots(5)$$

Where E_F is the combined end effect $E_{f1} + E_{f2} - E_{f1} \times E_{f2}$

In order to study the mechanism of the steady rise or fall of a drop it is necessary to either eliminate E_{f1} and E_{f2}, or to determine and allow for the quantity E_F.

If it were desirable to obtain either the formation or coalescence end effect it can be seen from Eq. (5) that it is necessary to eliminate one of these effects. If one effect is eliminated then Eq. (5) is simplified to

$$E_m = \frac{E_T - E_{f1}}{1 - E_{f1}} \quad \ldots\ldots(6)$$

or

$$E_m = \frac{E_T - E_{f2}}{1 - E_{f2}} \quad \ldots\ldots(7)$$

b) **Transfer mechanisms:**

During the steady fall or rise period of a drop heat or mass is transferred inside the drop by a transient process. The more important theoretical equations describing this transfer process are:

i) The Newman equation [13]: negligible continuous phase resistance and transfer in the drop by a molecular diffusion process:

$$E_m = \frac{C_2 - C_3}{C_2 - C^*} = 1 - \frac{6}{\pi^2} \sum_{n=1}^{\infty} \frac{e^{-\frac{Dn^2\pi^2 t}{r_d^2}}}{n^2} \quad \ldots\ldots(8)$$

ii) The Vermeulen equation [14] is an empirical equation closely approximating the Newman equation:

$$E_m = \left(1 - e^{-\frac{D\pi^2 t}{r_d^2}}\right)^{\frac{1}{2}} \quad \ldots\ldots(9)$$

or

$$-\ln(1 - E_m^2) = \frac{D\pi^2 t}{r_d^2}$$

By expanding $e^{-\frac{D\pi^2 t}{r_d^2}}$ in the right side, this equation may be simplified to

$$E_m = \frac{\pi}{r_d} D^{\frac{1}{2}} t^{\frac{1}{2}} \quad \ldots\ldots(9a)$$

It can be shown that this fits the Newman equation well for E_m values less than 0.5.

iii) The Kronig and Brink equation [15]: negligible continuous phase resistance and circulation within the drop:

$$E_m = 1 - \tfrac{1}{4} \sum_{n=1}^{\infty} B_n^2 \, e^{-\frac{\mu_n 16 D t}{r_d^2}} \quad \ldots\ldots(10)$$

iv) A modified Vermeulen equation has been shown by Korchinski [12] to represent the Kronig and Brink equation well:

$$E_m = \left(1 - e^{-\frac{R D\pi^2 t}{r_d^2}}\right)^{\frac{1}{2}} \quad \ldots\ldots(11)$$

where R had a value 2.25. Again, for E_m values less than 0.5 this may be modified to the following equation similar to (9a)

$$E_m = \frac{R^{\frac{1}{2}} \pi D^{\frac{1}{2}} t^{\frac{1}{2}}}{r_d} \quad \ldots\ldots(11a)$$

v) When there is appreciable resistance in the continuous phase the following equations by Jakob [16] describe the process:

$$E_m = \sum_{n=1}^{\infty} \frac{6}{Z_n^3} \frac{(\sin Z_n - Z_n \cos Z_n)^2}{(Z_n - \sin Z_n \cos Z_n)} \left(1 - e^{-\frac{D Z_n^2 t}{r_d^2}}\right) \quad \ldots\ldots(12)$$

where Z_n are the roots of the auxiliary equation (for heat transfer).

$$\frac{h_c r}{K} = 1 - nr \cot nr \quad \ldots\ldots(13)$$

vi) For a circulating drop with appreciable outside resistance the following equation is given and is based on Korchinski's premise that circulation streamlines act to effectively increase the molecular diffusivity by a factor R.

$$E_m = \sum_{n=1}^{\infty} \frac{6}{Z_n^3} \frac{(\sin Z_n - Z_n \cos Z_n)^2}{(Z_n - \sin Z_n \cos Z_n)} \left(1 - e^{\frac{R\, DZ_n^2\, t}{r_d^2}}\right) \quad \ldots(14)$$

For certain systems this factor R was found to be 2.25 by Korchinski [12].

c) Plotting methods

i) Resistance to transfer inside the drop: If there is resistance to transfer inside the drop, then Eq. (9) and (11) would indicate that the $-\ln(-E_m^2)$ should correlate against the group $\frac{D\pi^2 t}{r_d^2}$. The procedure here is to assume values of E_F and convert each E_T value to E_m which is then plotted as $1-E_m^2$ against $\frac{D\pi^2 t}{r_d^2}$ on semi logarithmic paper, or as $-\ln(1-E_m^2)$ against $\frac{D\pi^2 t}{r_d^2}$ on ordinary rectangular coordinates. The correct E_F value is that one which causes that data to lie on a straight line passing through zero. From the slope of the rectified line the modifier R [such as the 2.25 value of Eq. (11)] of the diffusivity can be obtained directly.

If sufficient data can be obtained at E_m values lower than 0.5 (for the water-cyclohexanol system in this study), Eq. (5) and (11a) can be combined to yield

$$E_T = (1 - E_F) \frac{R^{\frac{1}{2}} \pi D^{\frac{1}{2}}}{r_d} t^{\frac{1}{2}} + E_F \quad \ldots\ldots(15)$$

This equation indicates that E_T should be plotted against $t^{1/2}$ on rectangular coordinate paper. The intercept yields E_F and the slope may be used to obtain the correction factor R.

ii) Resistance to transfer in both phases: Examination of equation 14 indicates that there is no method similar to the above for plotting E_T data to obtain straight lines. If it is desired to estimate the end effect E_F and the exponent R from a set of data, a series of values of both E_F and R must be chosen until the data agree with the theoretical curves. This curve fitting technique will be illustrated by a sample calculation.

iii) Approximate method for obtaining E_F for either case: an empirical method for straightening data on rectangular coordinate plots uses

$$E_T' = (1 - A) E_T + A \quad \ldots\ldots(16)$$

where A is a constant with a recommended value of 0.80. Curved plots of E_T against t are considerably straightened and the intercept of the E_T' against t can be used to estimate the total end effect:

$$\text{intercept} = (1 - A) E_F + A \quad \ldots\ldots(17)$$

Although limited in accuracy, this method may be useful and will be illustrated by a sample calculation.

iv) Checking a suspected mechanism: Eq. (5) may be rearranged to give

$$(1 - E_T) = (1 - E_m)(1 - E_F) \quad \ldots\ldots(18)$$

$$\text{or } \ln(1 - E_T) = \ln(1 - E_m) + \ln(1 - E_F) \quad \ldots\ldots(19)$$

Since E_F is independent of time t, differentiating yields

$$\frac{d \ln(1 - E_T)}{dt} = \frac{d \ln(1 - E_m)}{dt} \quad \ldots\ldots(20)$$

This equation indicates that at any time the slope of the $\ln(1-E_T)$ curve is the same as the slope of a $\ln(1-E_m)$ curve. Hence, on semilog plots, comparisons of experimental data with theoretical equations may be made regardless of the magnitude of the combined end effects, E_F.

Illustrations of the above methods

Tables 1 to 4 show typical mass transfer data obtained by Hamielec [17]. By using aluminum particles suspended in the drops the runs of A, A°, and C were shown to be circulating while the drops in series B were oscillating.

TABLE 1

MASS TRANSFER DATA FOR THE WATER – n-BUTANOL SYSTEM AT 25° C. SERIES A°

Contact time (seconds)	E_T	E_m for $E_F = 0.300$
1.2	0.442	
1.2	0.435	0.199
3.0	0.503	
3.0	0.507	0.293
5.0	0.558	
5.0	0.551	0.365
6.2	0.590	
6.2	0.590	0.415

The drop diameter was calculated to be 0.00982 ft. The correction factor for circulation, R = 7.69

TABLE 2

MASS TRANSFER DATA FOR THE WATER – n-BUTANOL SYSTEM AT 25°C. SERIES B

Contact time (seconds)	E_T
1.0	0.365
1.5	0.421
2.4	0.494
3.5	0.553
4.6	0.598
6.0	0.650
7.0	0.685

The drop diameter was calculated to be 0.0124 ft. The correction factor for circulation, R = 29.6

TABLE 3

MASS TRANSFER DATA FOR THE WATER – CYCLOHEXANOL SYSTEM AT 25°C. SERIES A

Contact time (seconds)	E_T	E_m for $E_F = 0.150$
2.0	0.207	
2.0	0.195	0.060
10.0	0.270	
10.0	0.258	0.134
20.6	0.321	
20.6	0.321	0.201
30.0	0.357	
30.0	0.362	0.247

The drop diameter was calculated to be 0.0184 ft. The correction factor for circulation, R = 2.26.

TABLE 4

MASS TRANSFER DATA FOR THE WATER – CYCLOHEXANOL SYSTEM AT 25°C. SERIES C

Contact time (seconds)	E_T	E_m for $E_F = 0.110$
3.0	0.188	
3.2	0.181	0.084
9.8	0.222	
10.0	0.222	0.126
17.8	0.285	
17.6	0.289	0.199
26.4	0.320	
26.4	0.320	0.236

The drop diameter was calculated to be 0.0224 ft. The correction factor for circulation, R = 2.88.

In Figure 4 the data of Table 2 for oscillating drops are shown. The E_M values were obtained by Eq. (5) from the tabulated E_T values using the assumed values of E_F shown. It is seen that as larger E_F values are used the data is straightened and a line through this data is made to pass through zero. The correct E_F is estimated to be 0.135. From the slope of the line corresponding to this E_F value the effective diffusivity was found to be 28.3 x 10^{-8} ft²/sec. or 29.6 times the molecular diffusivity.

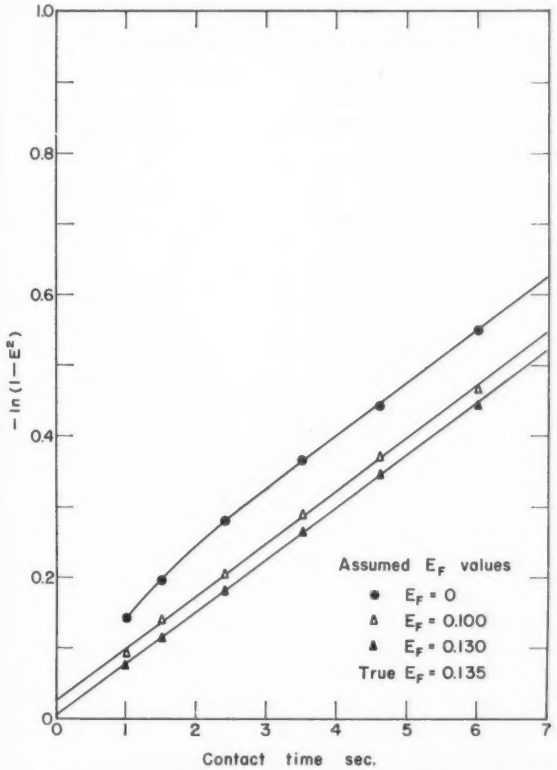

Figure 4—Observed and corrected mass transfer data for the water-n-butanol systems, Series B (Table 2) employing an end effect technique indicated by equation 9.

In Figure 5 the data of Table 3 are plotted as E_T against $t^{1/2}$ in accordance with Eq. (11a). The straight line has been extrapolated back to zero time to yield an E_F value of 0.150. From the slope of this line the R value was found to be 2.26.

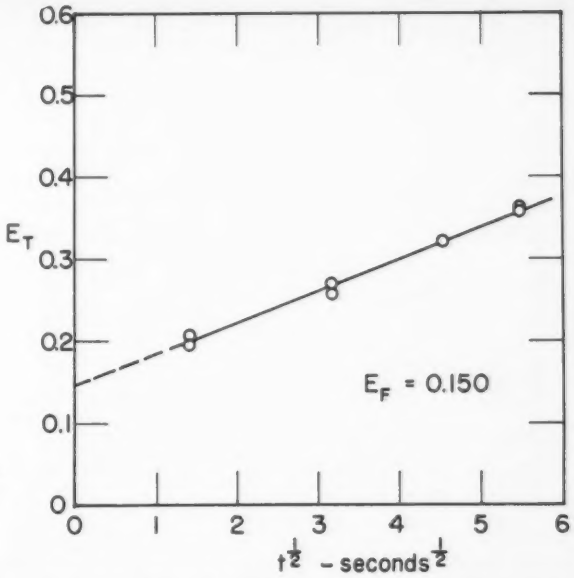

Figure 5—Observed mass transfer data for the water-cyclohexanol system, Series A (Table 3) exhibiting an extrapolation technique indicated by Equation 15.

The data of Tables 1 and 4 may be plotted on graphs similar to Figures 4 and 5 to obtain the R values indicated.

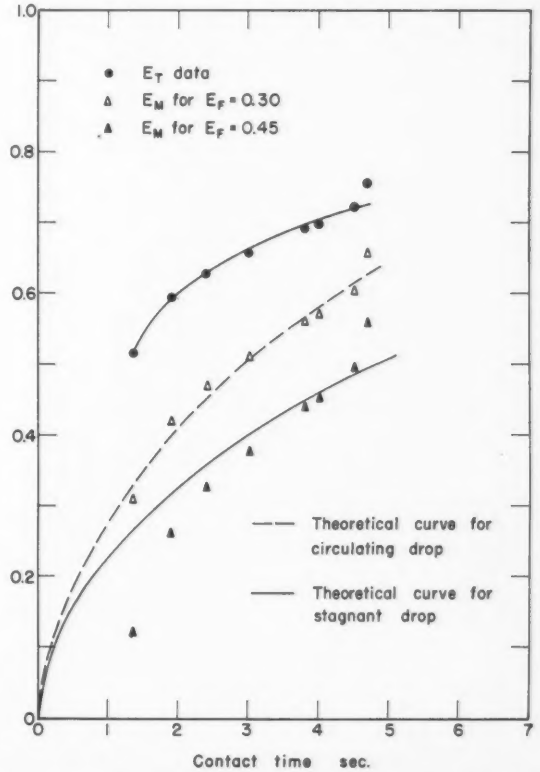

Figure 6—Observed and corrected heat transfer data for the bromobenzene-aqueous glycerine solution system (Table 5) exhibiting a curve fitting technique.

TABLE 5
HEAT TRANSFER DATA FOR BROMOBENZENE DROPS BEING COOLED BY FALLING THROUGH GLYCEROL SOLUTIONS

E_T	Contact time (seconds)
0.516	1.35
0.594	1.90
0.628	2.40
0.657	3.00
0.691	3.80
0.698	4.00
0.722	4.50
0.757	4:68

The drop diameter was calculated to be 0.635cm. The correction factor for circulation, R = 2.25

In Figure 6 the theoretical equation of Jakob for the cooling of non circulating drops [Eq. (12)] and the modified equation [Eq. (14)] using R = 2.25 have been plotted. The E_T data of Table 5 and the corresponding E_M data obtained using the assumed E_F values indicated are plotted as points. It is seen that as increasing E_F values are used the data points are moved downward. At $E_F = 0.30$ the data became superimposed on the Eq. (14) line. Within the accuracy of the data theoretical lines for other R values of Eq. (14) did not fit the data regardless of E_F values used.

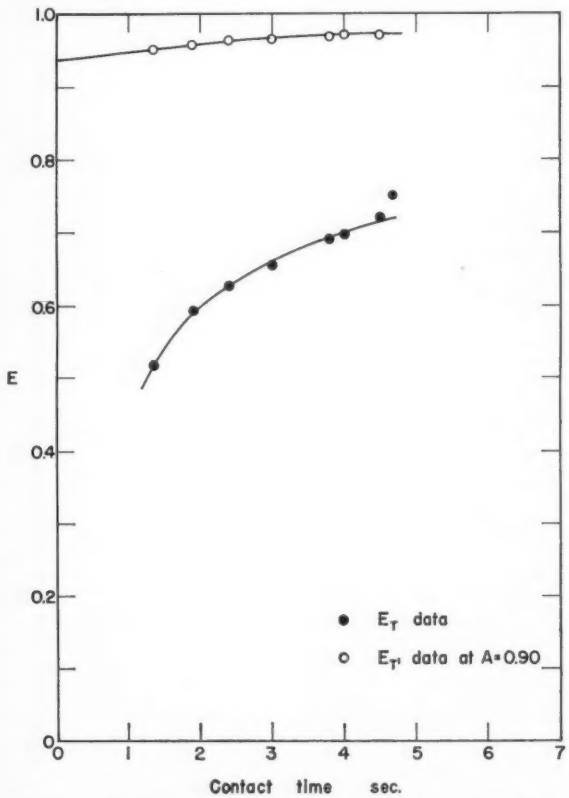

Figure 7—Observed heat transfer data (Table 5) indicating an extrapolation technique for estimating the order of magnitude of end effects present.

Finally, Figure 8 illustrates the comparison of data with theoretical equations. In this diagram it is easily seen that the experimental curve is parallel to the predicted curve of the Kronig-Brink equation. This indicates that

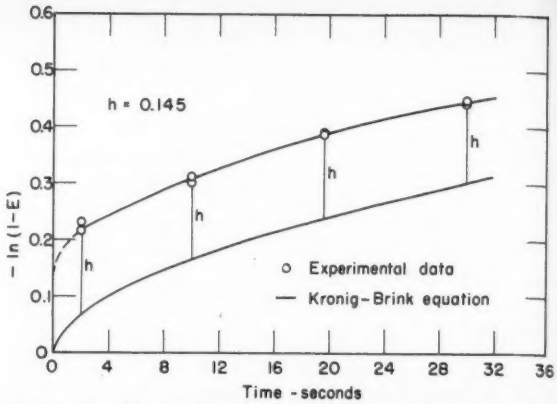

Figure 8—Observed mass transfer data for the water-cyclohexanol system, Series A (Table 3), exhibiting a mechanism test.

the Kronig-Brink equation holds for the steady fall period over the range of the experimental data.

Contact time for mass and heat transfer studies

It should be noted that the contact time for the steady fall or rise of a drop is less than the time required from drop break off to coalescence. The time to be used in the steady transfer equations should be

$$t = t^1 - \Delta t$$

where Δt is the time of the unsteady fall or rise period. Eq. (9) should be modified to

$$-\ln(1 - E_m^2) = \frac{D\pi^2 t^1}{r_d^2} - \frac{D\pi^2 \Delta t}{r_d^2}$$

This indicates that a negative intercept of value $\frac{D\pi^2 \Delta t}{r_d^2}$ should be expected when the data are plotted in the manner shown in Figure 4. However in the work encountered in this research to date, straight lines passing through the origin have represented the data well. It must be concluded that the time of the unsteady fall period is small compared to the time of the steady fall period.

Conclusion

This paper has attempted to define and to indicate simple calculation methods for obtaining the end effects for mass or heat transfer to drops or bubbles formed passing through a continuous medium from a nozzle to a settling area. Such end effects must be known before mechanisms of transfer during steady rise or fall periods can be investigated. Although the calculations are simple the present authors believe that they have been overlooked by most previous workers in this field.

Nomenclature

A = empirical constant
B = coefficient
C = concentration of dispersed phase
D = molecular diffusivity
D_E = effective diffusivity
E = a dimensionless number whose value is given by ($E_m \leq E \leq E_T$)
h = a dimensionless number = $-\ln(1 - E_F)$
h = film transfer coefficient
K = effective thermal conductivity inside drop.
R = correction for circulation or oscillation of drop phase = $\frac{D_E}{D}$, dimensionless
r = drop radius
Δt = time from point of drop release from the nozzle to the point when transfer mechanism of steady fall or rise period holds
t = contact time of drop for steady fall or rise period
t^1 = time taken by drop to strike the coalesced dispersed phase from the point of drops release from the nozzle

Greek Letters

μ = eigenvalue

Subscripts

1 = at column inlet
2 = beginning of the transfer mechanism of the steady fall or rise period
3 = point at which falling or rising drop strikes the coalesced dispersed phase
4 = at column outlet
T = overall
c = continuous phase
d = drop or dispersed phase
m = steady fall or rise period
n = term number in series sum
f_1 = end effect at entry end for dispersed phase
f_2 = end effect at exit end for dispersed phase

Superscripts

* = at equilibrium with respect to transfer of solute to or from dispersed phase

References

(1) Johnson, H. F., and Bliss, H., Trans. Am. Inst. Chem. Engrs. 42, 331, (1946).
(2) Sherwood, T. K., Evans, J. E., and Longcor, J. V. A., Ind. Eng. Chem. 31, 1144, (1939).
(3) Treybal, R. E., page 381, "Liquid Extraction", McGraw-Hill Publishing Co., New York, 1951.
(4) West, F. B., Robinson, P. A., Morgenthaler Jr., A. C., Beck, T. R. and McGregor, D. K., Ind. Eng. Chem. 43, 234, (1951).
(5) Licht, W., and Conway, C. J., Ind. Eng. Chem. 42, 1151, (1950).
(6) Licht, W., and Pansing, W. F., Ind. Eng. Chem. 45, 1151, (1950).
(7) Coulson, J. M., and Skinner, S. J., Chem. Eng. Sci. I No. 5, 197, (1952).
(8) Pang Sheng Li, Ph.D. Thesis, University of Washington (1953).
(9) Geankopolis, C. J., and Hixson, N. A., Ind. Eng. Chem. 42, 1141, (1950).
(10) Geankopolis, C. J., Wells, R. L., and Hawk, E., Ind. Eng. Chem., 43, 1848, (1951).
(11) Gier, T. E., and Hougen, J. D., Ind. Eng. Chem. 45, 1362, (1953).
(12) Calderbank, P. H., and Korchinski, I. J. O., Chem. Eng. Sci., 6, 65, 78, 1956.
(13) Newman, A. B., Trans. Am. Inst. Chem. Engrs. 27, 203, (1931).
(14) Vermeulen, T., Ind. Eng. Chem. 45, 1664, (1953).
(15) Kronig, R., and Brink, J. C., Appl. Sci. Res., A-2, 142, (1950).
(16) Jakob, M., "Heat Transfer," Vol. 1, Wiley, New York, 1949.
(17) Hamielec, A. E., M.A.Sc. Thesis, Chem. Eng. Dept., University of Toronto, 1958.
(18) Ward, D. M., M.A.Sc. Thesis, Chem. Eng. Dept., University of Toronto, 1957.

Acknowledgements

The following wish to acknowledge financial assistance for several sources during this work: A. E. Hamielec for an Ontario Research Foundation Scholarship, D. Ward for a California Standard Company Graduate Fellowship and A. Golding for a Union Carbide Research Fellowship.

* * *

LETTER TO THE EDITOR

New York, N.Y.

Editor, C.J.Ch.E.:

RE: Viscous Flow in Multiparticle Systems

This abstract reviews a series of theoretical studies which has resulted in achieving a better understanding of such phenomena as resistance to flow of fluids through beds, sedimentation of small particles and viscosity of suspensions. There are many systems both in nature and technology involving these types of motion. Examples of commercial applications include the separation of particles by centrifuging and sedimentation, filtration, flow of gases through vessels containing packed solids (kilns, gas producers and blast furnaces), and motion of particles and gases in catalyst contracting vessels.

In order to construct tractable mathematical models for the complicated flow systems involved, it is necessary to resort to some simplifications. Here, the inertia terms are omitted from the well known Stokes-Navier equations of motion, resulting in the so-called creeping motion equations. The operations noted above are often carried out in the Reynolds number range (based on particle diameter) of five or less and consequently are amenable to this assumption. The other important simplification is that the systems consist of uniform sized, spherical particles. The justification for these assumptions rests in part on the conciseness of treatment thus made possible and in part on the good agreement of results with available experimental data.

Essentially two techniques have been employed, namely the method of reflections and the unit cell. In the method of reflections the equations of motion are satisfied successively in each of the separate bounding surfaces including the container walls of a suspension. If the system is sufficiently dilute, rapid convergence is possible. The unit cell technique involves the concept that an assemblage can be divided into a number of identical cells, one sphere usually occupying each cell. The boundary value problem is thus reduced to a consideration of the behavior of a single sphere and its bounding envelope. This technique applies best where symmetry is more or less complete in the particle assemblage and thus is of greatest applicability in concentrated assemblages where the effect of container walls can be neglected.

An approximate theory for the behavior of dilute multiparticle systems suspended in a viscous fluid has been developed using the reflection technique [1]. This theory is based on a rigorous treatment for the case of a single sphere free to occupy any position, both axial [2] or off-axis [3] in a cylindrical tube. The results obtained include estimates of particle velocity and distribution as well as pressure drop due to fluid flow for several systems. They are in agreement with the qualitative data available.

In the case of the unit cell technique a novel approach has been developed on the basis that each of the particles is associated with an envelope of surrounding fluid which in turn is bounded by a "free surface". This model enables closed solutions of the hydrodynamic equations to be obtained. From these results rate of sedimentation or alternatively pressure drop can be predicted as a function of fractional void volume [4]. In the case of shearing motion similar solutions relate relative viscosity of a suspension to solids concentration [5]. Agreement with available data is very good without the use of any empirical constants for both resistance to flow and viscosity over a wide range of concentration.

In short, these studies have resulted in useful models for extension to more complicated cases, aside from their possible immediate application in practical correlations based on experimental data.

References

(1) Happel, J., and Brenner, H., A.I.Ch.E. Journal, 3 506, (1957).
(2) Happel, J., and Byrne, B. J., Ind. Eng. Chem. 46, 1181, (1954); corrections, ibid 49, 1029, (1957).
(3) Brenner, H., and Happel, J., J. Fluid Mechanics, 4, 195, (1958).
(4) Happel, J., A.I.Ch.E. Journal, 4, 197, (1958).
(5) Happel, J., J. Appl. Phys. 28, 1288, (1957).

John Happel,
College of Engineering,
New York University.

* * *

Received June 2, 1958.
Based on a talk presented with lantern slides before Local Sections of The Chemical Institute of Canada, January 1958.